DEVELOPING A NOVEL MIX DESIGN TECHNOLOGY FOR 'RAMMED EARTH' USING PULP MILL FLY ASH AS CEMENTITIOUS MATERIAL

by

Amin Ajabi Naeini

BSc, Isfahan University of Technology, 2011

MSc, Isfahan University of Technology, 2014

A THESIS SUBMITTED IN PARTIAL FULFILLMENT OF

THE REQUIREMENTS FOR THE DEGREE OF

MASTER OF APPLIED SCIENCE

in

THE COLLEGE OF GRADUATE STUDIES

(Civil Engineering)

THE UNIVERSITY OF BRITISH COLUMBIA

(Okanagan)

January 2021

The following individuals certify that they have read, and recommend to the Faculty of Graduate and Postdoctoral Studies for acceptance, a thesis/dissertation entitled:

Developing a Novel Mix Design Technology for 'Rammed Earth' Using Pulp Mill Fly Ash as Cementitious Material

submitted by Amin Ajabi Naeini in partial fulfillment of the requirements for

the degree of Master of Applied Science in Civil Engineering.

Examining Committee:

Dr. Sumi Siddiqua, School of Engineering

Supervisor

Dr. Ramy Saadeldin, Adjunct Faculty, School of Engineering

Supervisory Committee Member

Dr. Nima Latifi, Industry

Supervisory Committee Member

Dr. Rudolf Seethaler, School of Engineering

University Examiner

Abstract

Rammed earth (RE) is a traditional soil-based building material made by compressing a mixture of natural earth and binder ingredients in temporary frameworks. The modern RE uses 5 to 10% cement as a binder to meet the strength and durability requirements. Due to the CO_2 footprints associated with cement production, this research aimed to develop and assess innovative waste-to-product technologies and strategies for the transformation and effective utilization of pulp mill residues in the construction sector as a partial replacement for conventional Portland cement. For the experimental study, the as-received pulp mill fly ash (PFA) and a fly ash-based geopolymer synthesized by alkali-silicate activation method, were incorporated as cement substitutes in the RE mixtures. Initially, the local soil was collected and characterized by important index and engineering properties. The fly ash was procured from a local pulp mill, and its physico-chemical, mineralogical, and morphological characterization, as well as environmental impact, was identified. Further, the various mix designs of RE material incorporating local soil and different proportions of Portland cement, pulp mill fly ash, calcium bentonite, and alkali-silicate activator (a mixture of sodium silicate and sodium hydroxide solutions) were developed. The compacted RE specimens were cured and tested for 7-day and 28-day unconfined compressive strength (UCS) variations. The PFA and calcium bentonite-treated samples, as well as samples that were stabilized by the alkali-silicate activator, exhibited significant strength improvement. Further, the cured RE specimens were subjected to a standard freeze-thaw durability test to evaluate their frost resilience properties as a sustainable construction technique under extreme climatic conditions. The alkali-silicate activator-treated samples were highly unstable under extreme weathering conditions. On the other hand, the specimens treated with calcium bentonite and PFA retained their full strength under the freeze-thaw cycles. As a result, it was concluded that even though the alkali-silicate

activation of PFA improved the compressive strength of RE samples, this method is not durable in hard weathering conditions. Furthermore, treating RE specimens with PFA and bentonite was beneficial for the improvement of mechanical and durability properties of RE samples and can be a practical step towards the utilization of waste by-products.

Keywords: Rammed earth, Recycled pulp and paper fly ash, Calcium bentonite, Geopolymerization, Alkali-silicate activators, Compressive strength, Freeze-thaw durability.

Lay Summary

The pulp mill fly ash (PFA) is a wood-based combustion by-product collected in the electrostatic precipitators of the power boiler units during the pulp manufacturing process in the Kraft pulp mills. These environmentally massive wastes are generally discarded in the in-house landfills which incur approximately $25 to 50 per tonne ash. As a result, these industries are seeking more efficient, sustainable strategies to manage their wastes and thereby gain greater environmental and economical benefits. Based on the current understanding of pulp mill residues, the PFA has favorable characteristics to be potentially considered as an environmentally safe replacement for Portland cement in the construction sector. Therefore, this study aimed to find a novel solution for the utilization of recycled PFA into an inert value-added secondary material targeting its potential application in sustainable RE construction.

Preface

This thesis aimed at evaluating the suitability of pulp mill fly ash (PFA) for utilization in the RE materials. For this, the stabilization process was performed in two stages (1) effectiveness of alkali-silicate activator and (2) the effectiveness of calcium bentonite (Ca-bentonite) on the strength and durability performance of RE samples. The author's responsibilities included literature survey, overall planning of the research, performing laboratory tests, data organization and analysis, and thesis writing under the supervision of Dr. Sumi Siddiqua and the great help of Postdoctoral fellow Dr. Chinchu Cherian. The laboratory experiments were carried out in the Advanced Geomaterials Testing Laboratory, located at the School of Engineering. The Scanning electron microscopy (SEM) and energy-dispersive X-ray spectroscopy (EDS) analysis were conducted at the FiLTER - Fipke Laboratory for Trace Element Research, the University of British Columbia (UBC) Okanagan Campus. X-ray diffraction (XRD) test was conducted on the UBC Vancouver campus. Ethics approval from the UBC Research Ethics Board was not required for this study. While completing my master's program I was able to submit one technical paper to a peer-reviewed journal for possible publication and one paper for an international conference. The list of submitted and preparing papers related to this thesis is presented below.

- Ajabi, A., Siddiqua, S., Cherian, C., A Novel Mix Design Technology for Sustainable 'Rammed Earth' Using Pulp Mill Fly Ash Based Geopolymer as Cementitious Material, Journal of Construction and Building Materials (submitted).
- Ajabi, A., Siddiqua, S., Cherian, C., A Novel Mix Design for Wood Ash-incorporated Rammed Earth Material, Thirty-Sixth International Conference on Solid Waste Technology and Management 2021, March 14-17 *Online* (accepted).

Table of Contents

List of Tables

List of Figures

List of Abbreviations

ASTM	American Society for Testing and Materials.
Al	Aluminum
Ba	Barium
BC	British Columbia
Ca	Calcium
CASH	Calcium aluminate silicate hydrate
CRM	Certified reference material
CSH	Calcium silicate hydrate
Cu	Copper
EDS	Energy dispersive spectroscopy
EPA	Environmental protection agency
FTIR	Fourier transform infrared spectroscopy
G	Specific gravity
GGBS	Ground granulated blast furnace
ICP-MS	Inductively coupled plasma-mass spectrometry
LCCA	Life cycle and cost analysis
MDD	Maximum dry density
NMC	Natural moisture content
OMC	Optimum moisture content
P	Phosphorus
Pb	Lead
PC	Portland cement

PFA	Pulp mill fly ash
PSD	Particle size distribution
RE	Rammed earth
SEM	Scanning electron microscopy
TC	Total carbon
UCS	Unconfined compressive strength
USCS	Unified Soil Classification System
XRD	X-ray diffraction analysis

Acknowledgments

I would also like to express my sincere gratitude to my supervisor Dr. Sumi Siddiqua for the continuous support of my study and related research, for her patience, motivation, and immense knowledge. Besides my advisor, I would like to thank the rest of my thesis committee for their helpful advice. I also have to mention my great appreciation for the help and support I received from Dr. Chinchu Cherian. Her valuable inputs kept me motivated during my research. I would like to thank my fellow students in the Geomaterial Research Laboratory for their support. My sincere thanks also go to Kim Nordstrom and Michelle Tofteland for their great help with my laboratory experiments.

I owe my profound gratitude to my beloved family, especially my parents, for their supports throughout my life. Moreover, I wish to express my special appreciation to my wife and best friend, Sadaf. None of this would have happened without her support and continuous encouragement.

Dedicated

to

My dear parents

Ai & Safa

And my beloved wife

Sadaf

Chapter 1: Introduction

1.1 Overview

In this era of globalization and urbanization, the rapidly growing building sector is one of the most resource-intensive industries by consuming more than 40% of the world's global energy and resources. Furthermore, it is a major contributor to environmental pollution by generating an enormous amount of waste (Akadiri et al., 2012). The conventional construction methods using Portland cement concrete (PCC) adversely impacts the environment in terms of harmful CO_2 emissions during Portland cement (PC) manufacturing processes as well as during the building construction activities and its entire life cycle. These emerging issues have led the researchers to focus on the revival of traditional earthen construction methods including rammed earth (RE) walls, earth bricks, and compressed earth blocks, with sustainable and energy-saving criteria as key drivers (Maniatidis and Walker 2003; Morel et al., 2007; Burroughs 2008, 2010; Siddique and Barreto, 2018). The conventional RE structures are constructed on-site by compacting layers of local soil mixture consisting of gravel, sand, clay, and silt, in a temporary framework (Siddiqua and Barreto, 2018). These structures have potentially low manufacturing impacts since the available clay mineral content acts as natural binders between soil grains, and hence, they are commonly referred to as "un-stabilized rammed earth".

1.2 Motivation

The establishment of the RE construction technique dates back to 7500 BCE (Berge, 2009); however, there are several problems associated with un-stabilized RE including low strength and durability. To overcome these problems, the modern RE construction practiced the addition of 5 to 10% PC to act as an efficient stabilizing agent (Bui et al., 2014; Kariyawasam and Jayasinghe,

2016). The cement stabilized RE possesses superior strength and durability properties essentially required to meet the construction standards. Nevertheless, the growing concerns regarding cement production and associated greenhouse gases emissions, triggered researchers to search for more innovative, sustainable, and eco-friendly binder materials for RE stabilization.

Several recent studies investigated the viability of employing secondary raw materials from industrial waste streams with low embodied energy (viz., coal fly ash, rice husk ash, sludge ash, sawdust ash, etc.) as alternative resources for PC in construction (Ganesan et al., 2007; Chusilp et al., 2009; Siddique, 2009, 2012; Jaiswal and Lal, 2017; Leong et al., 2018; Teixeira et al., 2019). The beneficial uses of industrial wastes will not only provide inexpensive and eco-friendly construction strategies but also significantly reduce the stockpiles of these wastes and mitigate ancillary environmental impacts (Faubert et al., 2016). However, using these by-products as a substitute for PC has certain drawbacks such as slow initial strength gain and seasonal limitations. The previous researches established that these weaknesses can be overcome through chemical activation techniques such as alkaline activation which is also termed as geopolymerization (Majidi, 2009; Palomo et al., 2014; Singh et al., 2015; Sotelo-Piña et al., 2019).

The geopolymerization process consists of sequential steps such as the dissolution of alumino-silicate bonds in the precursor substances, which are rich in amorphous Si and Al (i.e. fly ash). This process takes place due to the alkali attack followed by polymerization and growth of amorphous three-dimensional alumino-silicate materials or geopolymers (Sabrin et al., 2019). These geopolymers are large inorganic molecules, characterized by higher particle size and reduced exposed surface which imparts enhanced cementitious properties (Li et al., 2016; Leong et al., 2018). However, there are not many studies that have assessed the effectiveness of

geopolymerized fly ash as a binder in RE (Cristelo, et al., 2012a; Bui et al., 2018; Meek and Elchalakani, 2019).

The pulp and paper mill fly ash (PFA) is a wood combustion by-product with low embodied energy generated during the pulp manufacturing process in the Kraft pulp mills, and these environmentally massive wastes are generally discarded in the in-house landfills (Ochoa de Alda, 2008; Cherian and Siddiqua, 2019). For instance, the pulp and paper industries produce more than 1 million tonnes of PFA per year and spend approximately $25-50 per tonne of ash for its transportation and disposal at the landfills. The statistical studies predict significantly increasing production of fly ash in future years owing to the continual growth of pulp and paper industries (Lamers et al., 2018; Simão et al., 2018). As a result, these industries are seeking more efficient, sustainable strategies to manage their wastes and thereby gain greater environmental and economical benefits. Based on the current understanding of pulp mill residues, the PFA has favorable physico-chemical and ecotoxicological properties to be potentially considered as an environmentally safe replacement for PC in the construction sector (Ahmadi and Al-Khaja, 2001; Toller et al., 2009; Hall et al., 2012; Faubert et al., 2016). Due to the high percentages of amorphous silica, alumina, and calcium oxide present in wood ash, it is also suitable as a precursor to synthesize geopolymer binders of high mechanical performance. Some previous studies developed new approaches to assess wood ash as a supplementary cementitious material for cement and concrete systems (Udoeyo et al., 2006; Chusilp et al., 2009; Grau et al., 2015), as a chemical binder for soil stabilization (Šķēls et al., 2016; Murmu et al., 2020) and aggregate in pavement construction (Chauhan et al., 2008; Edeh et al., 2014).

1.3 Objectives

The key motivation of this study is to find a novel solution for the valorization of recycled PFA

into inert value-added secondary material, which is targeting its potential application in sustainable RE construction. This research project is designed and implemented to synthesize an eco-efficient binder of high mechanical performance from PFA at first by alkali-silicate activation at ambient temperature (~22 °C), and at the second stage by adding calcium bentonite (Ca-bentonite), to be used in the stabilized RE material. For attaining this goal, the following objectives must be met:

1- Preparing different design mixtures of composite RE material using locally available aggregates, and various combinations of PC, PFA, activator solutions, and Ca-bentonite.
2- Determining the most efficient design mix based on the comparative mechanical and durability performance of different mixtures, particularly in terms of variations in the strength, stiffness, and frost resilience properties after 28 days of standard moist curing.
3- Comprehend the underlying stabilization mechanisms as well as substantiate macro-level variations in strength and durability properties.

These objectives are accomplished by implementing the following primary tasks:

1- Characterization of materials including soil, cement, Ca-bentonite, and PFA.
2- Formulating RE mix designs with different percentages of stabilizers and determining their compaction characteristics.
3- Evaluating the mechanical performance of different RE mixtures in terms of uniaxial compressive strength after 7 days and 28 days curing.
4- Investigating the frost resilience properties of stabilized RE material after 28-days curing by standard freeze-thaw durability tests.
5- Conducting the micro-level examination of stabilized RE specimens with the aid of scanning electron microscopy (SEM) coupled with energy dispersive spectroscopy (EDS) and Fourier transform infrared spectroscopy (FTIR) analysis.

6- Assessing the environmental compatibility of the optimized RE material by performing the standard leachate analysis and measuring trace element concentrations.

1.4 Novelty of research

To the best knowledge of the author, no significant research has been conducted in the past to investigate the potential application of PFA in sustainable earthen construction as a substitute for PC, even though the environmental risk characterization assessments regarded it as a non-hazardous commercial waste over many decades. It is anticipated that the beneficial utilization of PFA and secondary products in RE material will help to further reduce the constructional and operational CO_2 emissions, and it will ultimately enable us to take one step forward in the growing high-tech, green-focused industry. Ultimately, the overall goal of this research is to develop and assess innovative waste-to-product technologies and strategies for the transformation and effective utilization of pulp mill residues in the construction sector.

1.5 Thesis organization

This dissertation consists of five chapters, as follows:

Chapter One provides an introduction to environmental issues and the importance of choosing a sustainable construction method. Further, it highlights the importance of using PFA as an eco-friendly binder in RE. Besides, this chapter underlines the objectives of this study and the steps needed to achieve them.

Chapter Two reviews the literature on different methods of evaluating the durability performance of earthen material structures. Further, it provides detailed background on geopolymerizations in RE. Then, the specification of clay materials, as well as bentonite and its performance in RE, is discussed.

Chapter Three provides the methodology for attaining the objectives of this study. It describes the methods implemented in this study for the characterization of soil, PFA, cement, and Ca-bentonite. The details on the physical, mechanical, and durability experiments on the RE samples were presented. It also points out the information regarding micro-level experiments that were performed on RE samples including FTIR, SEM-EDS, as well as the leachate analysis for environmental risk assessment.

Chapter Four presents the important results of the performed tests. The effect of different mix designs on the physical, mechanical, and durability of the RE samples is discussed. The SEM-EDS result along with FTIR data are analyzed.

Chapter Five covers a summary of this dissertation and introduces the outcomes of each objective. Further, this chapter presents the study limitations and recommendations for future studies.

Chapter 2: Literature Review

2.1 Research background on rammed earth

RE walls are constructed by compacting different layers of soil mixture including gravel, sand, clay, and silt on their optimum moisture content (OMC). Multiple challenges are associated with rammed earth applications, for example, their slow strength gain, or their durability (Jayasinghe and Kamaladasa, 2007; Ma et al., 2016). However, there are remaining of these structures in Portugal, Japan dating back to more than 500 years ago (Hall and Djerbib, 2004; Silva et al., 2013; Kariyawasam and Jayasinghe, 2016). Traditionally, clay was utilized as the binding agent for soil particles while other binding agents are utilized more recently to improve strength and durability.

There are multiple methods for stabilizing RE structures, for example, chemical, physical, and mechanical stabilizing methods. Chemical stabilizing refers to the method in which the addition of binding agents e.g., cement, calcium lime, and fly ash can improve the strength characteristics. Physical stabilization refers to the taking of soil with proper particle size or having a suitable mix of soil particles (e.g., gravel, sand, silt, and clay). Furthermore, mechanical stabilizing refers to the application of a pneumatic rammer or a manual one for soil compaction (Bui et al., 2014; Kariyawasam and Jayasinghe, 2016). As discussed earlier one of the critical concerns related to RE structures is their durability. To address that problem, lots of studies have been performed on the different aspects of durability. In the following section, a review of some research studies in three categories comprising rammed earth walls durability in different weather conditions, thermal properties of rammed earth walls, and mechanical characteristics of rammed earth structures area will be provided.

2.1.1 Rammed earth durability in different weather conditions

Heathcote (Heathcote, 1995) went through some rainfall parameters that can affect the durability of rammed earth walls, for example, rainfall intensity, the angle of rainfall, and wall roughness. He also provided a review on the approaches of durability testing consist of wire brush test, spray test, drip test, and wet-to-dry strength approach. Furthermore, he applied the spray test on 12 bricks with different cement contents and compared the results with the wet-to-dry strength ratio. Finally, he concluded that the ratio of wet-to-dry strength should be used as an indicator of earth wall durability. Ogunye and Boussabaine (Ogunye and Boussabaine, 2002) developed a device that imitates natural rainfall conditions. The device was able to evaluate the durability of the walls and bricks by simulating rainfall conditions soil blocks. Multiple samples were stabilized with different binding agents including cement, lime, and lime-gypsum in different proportions. The block samples had different values of soil mass loss between 0.26- 4.0% that was considered in the standard limit and the data collected under the artificial rainfall had a reasonable correlation with natural rainfall. Guettala et al. (Guettala et al., 2006) constructed eight walls using RE bricks with different stabilizers. The bricks contained different portions of soil, sand, cement, lime, and resin. All the assessments were completed under a natural weather condition. The laboratory experiments including compressive strength, capillary absorption, total absorption, wetting and drying test, freezing and thawing, spray test, and water strength coefficients were conducted on the samples. The stabilized samples were more durable compared with samples with no stabilizer. Finally, they suggested that stabilizing bricks with 5% cement and a compacting pressure of 10 MPa would give satisfying durability for bricks containing sandy clay. Hall (Hall, 2007) utilized a climate chamber to evaluate the performance of RE walls. This chamber could assess full-scale building elements and evaluate the rainfall penetration based on British Standard BS 431-2 1970.

The chamber had a simulator with two parts containing the design side, and the climate side. The function of the design part was to simulate the interior part of the building. It was capable to maintain the inside room condition within the standard limit. On the other hand, the climate side was able to apply different weather conditions on the exterior parts. Moreover, the chamber could determine the temperature, relative humidity, and some other weather elements. They applied multiple test phases to simulate low/high-velocity rainfalls. Furthermore, they installed different types of sensors for collecting variations in temperature, liquid moisture content, and relative humidity over several testing conditions. They figured out that the wall durability performance was affected by the temperature variations. Eventually, it was observed that all the cement-stabilized walls had a promising performance. Bui et al. (Bui et al., 2009) conducted a study to evaluate the durability of RE walls for 20 years in a natural weathering condition. The average annual rainfall in the area was 1000 mm and the maximum wind speed was 21 mm/s. They built walls in 1985 in the French Alpine valley. There were built three types of rammed earth walls including fine RE (fine soil), medium RE (a mixture of fine RE and non-argillaceous soil), and the stabilized medium RE (medium RE stabilized with 5% lime). The erosion was measured using the stereo-photogrammetric method. In this method, the photos that were captured from two sides of the wall were analyzed by a stereoscope. After 20 years, lime stabilized RE walls exhibited a 2mm erosion which was about 0.5% of the wall thickness. It was concluded that the stabilization was enough to protect the wall and there was no need to use plaster. Also, the unstabilized walls had the erosion about 1.6% of wall thickness that exhibited the potential for the application of unstabilized rammed earth walls in the same weather condition. Authors concluded that the RE walls do not need to be stabilized with lime or cement in the similar weather condition, due to the problems associated with their recycling process and accessibility in some countries. Furthermore,

they suggested that new types of experiments are needed to be developed to evaluate the durability of RE walls based on the specific climate conditions they are located in. In another study, Arrigoni et al. (Arrigoni et al. , 2017) evaluated the durability of stabilized RE under wetting-drying cycles. The unconfined compressive strength as well as microstructural analysis were performed to assess samples. The samples were stabilized with cement, fly ash and calcium carbide residue and the results exhibited the improvement on the mechanical properties of stabilized samples after applying the wetting-drying cycles. Authors concluded that the use of waste materials is an effective method for RE stabilization. Beckett et al. (Beckett et al., 2020) provided a framework for evaluating the durability performance of RE under the water exposure by reviewing previous works. Their framework presented a range of experiments to assess the durability of RE walls in different environmental conditions.

2.1.2 Thermal performance of rammed earth structures

The thermal performance of RE structures was evaluated by several researchers. Taylor and Luther (Taylor and Luther, 2004) investigated the thermal characteristics of RE structures. They evaluated the heat flux in an office that was constructed by RE walls with 300 mm thickness. The heat flux data were collected using several thermistors installed in different spots in the office. They analyzed the performance of the walls by evaluating the energy transfer in the office through the walls during the working hours. Their collected data exhibited that the heat exchange through the external wall to the office was extremely limited and the heat was absorbed by the internal wall, which helped cooling down the internal airspace. Taylor et al. (Taylor et al., 2008) evaluated the thermal comfort and energy use of a building constructed with RE walls employing two methods. First, they utilized a questionnaire to find out the viewpoint of building occupants about their temperature sensations. Also, they measured the internal and external heat exchanges of walls

with transducers and used a model to describe the thermal comfort zone. Their measurements were aligned with the questionnaire and confirming that during the summer the building is too hot and during the winter is too cold. It was also noticed that the RE building uses more energy for heating than other buildings in the same location. Furthermore, they simulate a model to anticipate temperature in the summer and winter to improve building energy efficiency. Finally, they suggested that the design change and a modern control policy can be helpful. Hall and Allinson (Hall and Allinson, 2009) evaluated the hygrothermal properties of stabilized RE. First, they specified multiple hygrothermal properties of stabilized RE structures such as moisture storage function, vapor permeability, liquid conductivity, thermal conductivity, and specific heat capacity. Then, they evaluated these properties in three different RE mix designs. They concluded that the hygrothermal properties of stabilized RE are designable and related to compaction energy and particle size distribution (PSD) of samples. Soebarto (Soebarto, 2009) evaluated the thermal performance of two houses with RE walls and compared it with the performance of another house with insulated RE walls. Initially, they measured the temperature of houses to simulate the thermal performance. The simulation exhibited that the temperature variations of houses during the summer were insignificant. However, the results from the winter revealed that the house with insulated RE walls was 5°C warmer than the other houses with only RE walls. Dong et al. (Dong et al., 2014b) performed a research study on multiple strategies to reduce the heat exchange in structures with uninsulated RE walls in different climate zones of Australia. Primarily, they described multiple options that were established in the national construction code to improve the thermal resistance of RE walls. These options were including insulating rammed earth walls, star rating requirements, and passive solar heating strategies. Furthermore, they used home energy rating software to simulate the energy load of RE houses in different climate zones of Australia.

They investigated the effect of five factors, including glazed area, shading, wall thickness, ventilation, and window type. Finally, they provided recommendation for the design of uninsulated RE houses in each climate zone to meet the Australian building standards. Dong et al. (Dong et al., 2014a) in another study evaluated the effect of window size, shading, ventilation rate, and wall thickness on the inside temperature of RE houses. They simulated houses with uninsulated RE walls in different climate zones. They found out that it is possible to improve the thermal comfort in a RE house with a natural ventilation system, by considering multiple design parameters based on the specific climate condition. Soudani et al. (Soudani et al., 2017) monitored thermal data from an uninsulated RE house to assess its performance in different seasons. They installed multiple sensors inside (during the construction) and on the surface of the RE walls to measure temperature, relative humidity, and water content. Furthermore, they measured the temperature and relative humidity indoor and outdoor. Based on their measurements, the house had a satisfying comfort in the summer and acceptable energy performance in the winter. Besides, they figured out that the thermal behavior of RE walls is related to the water content of the wall. In a recent study, Jain et al. (Jain et al., 2019) focused on improving the thermal performance of RE bricks. They prepared samples of RE bricks with clay, sand, and rubber and measured the thermal resistance of samples. The experiments were based on measuring the temperature at the top of the sample while it is on a hot plate and heat is applied from the bottom. Also, they performed a finite element analysis of the thermal stress and heat transfer of rammed earth samples to evaluate the effect of shape, orientation, size, and filler volume fraction of rubbers. Upon their analysis, they figured out that the volume fraction of fillers is the most important parameter to improve the thermal resistance. Besides, they found the shape of the filler as a key factor for increasing the thermal resistance.

2.1.3 Mechanical characteristics of rammed earth structures

In this category, some studies are more focused on the scale effect, load direction, and finding a correlation between strength parameters. For example, Maniatidis and Walker (Maniatidis and Walker, 2008) performed multiple experiments on RE samples, including small scale compression test, large scale prism test, and full-size column test under concentric and eccentric axial load. Moreover, they used an analytical model to anticipate the structure capacity under different loading conditions. Their prediction of high load eccentricities for column failure load did not match with the experimental results. The reason was due to the ignorance of the suppressed cracking in their analysis. Additionally, they obtained different results for the samples with the same contents in the small-scale compression test, full-scale prisms, and columns tests. The resulted inconsistency was attributed to the difference in particle size distribution and the compaction energy of samples.

Jaquin et al. (Jaquin et al., 2009) evaluated the suction effect in the compressive strength of RE samples. They performed six unconfined compression tests on RE samples with constant water content. The samples were dried to reach the targeted water content prior to the tests. The results indicated that water content limits strength improvement. Bui et al. (Bui et al., 2009) investigated the mechanical performance of RE walls in three scales of in situ walls, representative volume element, and compressed earth blocks. The approach of the study was to measure the elastic modulus of samples in three scales. For the in-situ wall, they determined elastic modulus employing a finite element model. For the next two scales, they used an unconfined compressive strength test in the laboratory to calculate elastic modulus. The results indicated similar values for the second and third scales, while in-situ dynamic measurements exhibited the highest value of elastic modulus. The authors contributed these results to the perfect layer adhesion of the modeled RE wall.

In another study, Bui and Morel (Bui and Morel, 2009) investigated the anisotropy of RE structures on the two scales of the representative volume element (REV) and microscopic. For the REV scale, they applied loading-unloading cycles and uniaxial compressive test in two directions. Their results indicated that the RE could be assumed as an isotropic material in the REV scale if their layers do not separate. For the microscopic scale, they modeled samples with the same characteristics of the REV scale to evaluate the possibility of using microscale samples in the laboratory. The results for compressive strength, loading-unloading, and failure modulus were consistent with the results of REV scale samples. Bui et al. (Bui et al., 2014) performed multiple experiments to estimate the tensile strength of RE structures. Later, they determined the relation between compressive and tensile strength. Based on their results they could confirm the isotropic assumption for RE material. Later, they applied local failure tests on two wallets to investigate the effect of concentrated load on RE walls. Furthermore, they successfully modeled the failure surfaces of the walls using a finite element model.

Other than the approaches reviewed in this category, some studies are more focused on the effect of different stabilizers like date palm fibers (Taallah et al., 2014), wool fiber (Aymerich et al., 2012), and polymer (Marais et al., 2015) on the strength characteristics of rammed earth samples. For example, Siddiqua and Barreto (Siddiqua and Barreto, 2018) studied the effect of using industrial by-products including calcium carbide residue and fly ash in RE samples. The evaluation was performed by conducting the uniaxial compressive strength of RE samples after their curing time. The results from SEM-EDS were compatible with the results of compressive strength tests.

Liu et al. (Liu et al., 2018) investigated the durability, thermal properties, and strength of RE samples filled by steel slags. They conducted wetting and drying cycles, frost resistance, and water

resistance tests to evaluate the durability of RE samples with different stabilizer content. Also, they measured the thermal conductivity of samples with different percentages of steel slags to assess the thermal performance. For the strength characteristics, they performed a compressive strength test on samples after 14, 28, and 60 days of curing. They figured out that the addition of steel slags will enhance durability and compressive strength while reduces the thermal performance of samples. In another study, performed by Toufigh and Kianfar (Toufigh and Kianfar, 2019) the effect of introducing different stabilizers on the strength and thermal performance of RE samples were assessed. The stabilizers in this study were consist of cement, pozzolan, micro silica, fiberglass, guar gum, and phase change materials. Authors evaluated the influence of each material through conducting an unconfined compressive strength test, tensile splitting test, ultrasonic test, wire brush test, thermal conductivity, humidity, and drying shrinkage test.

2.1.3.1 Geopolymerization in rammed earth

Geopolymer characteristics

Davidovits is considered as the first person who introduced the term ‘Geopolymer’. The reaction of an alkali solution with alkali-activated materials containing alumino-silicate will form geopolymers. Some alkali-activated materials are naturally formed (metakaolin) and some are created from industrial wastes (fly ash, blast furnace slag). Geopolymer is synthesized during a process named geopolymerization in which a sequence of SiO_4 and AlO_4 are connected like a chain (Majidi 2009). A schematic view of this process is demonstrated Figure 2.1.

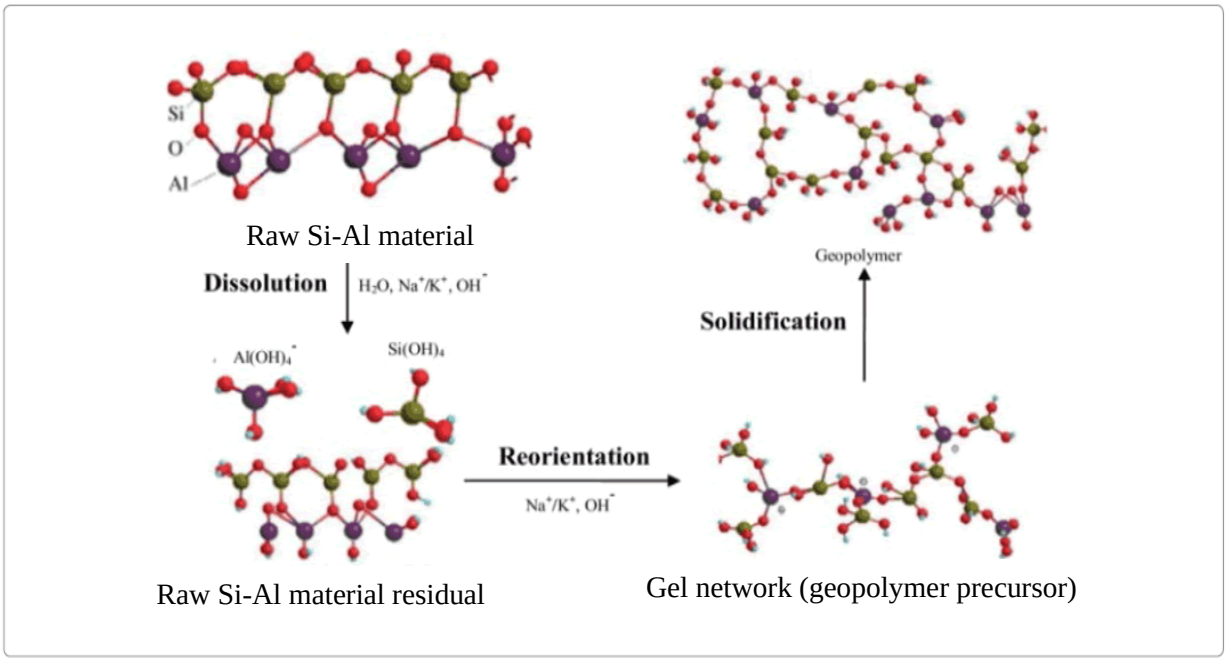

Figure 2.1 The schematic view of geopolymerization (Hameed and Rawdhan, 2017).

Reactions in the geopolymerization process are presented in equations 1 and 2.

$$(Si_2O_5Al_2O_2)_n + H_2O + OH^- \rightarrow Si(OH)_4 + Al(OH)^{4-} \quad (1)$$

$$Si(OH)_4 + Al(OH)^{4-} \rightarrow (-Si(-O-)(-O-)-Al(-O-)(-O-)-)_2 + 4\,H_2O \quad (2)$$

The other materials used to form geopolymers are activators. The chemical composition of activators (anions and cations) affects the geopolymer characteristics. The most common anions which are mixed with materials to create an alkali environment are hydroxides, carbonates, silicates, and sulfates. Also, activators such as sodium hydroxide, sodium silicate, potassium hydroxide, and potassium silicate are normally applicable for the activation of aluminosilicates (Palomo et al., 2014; Singh et al., 2015).

Advantages of geopolymers

The Portland cement has boundless applications in the construction industry, such as building materials, transportation systems, and infrastructures. In contrast to these major applications, there

are disadvantages including a high rate of energy consumption during the production process, low level of chemical resistance, and a high possibility of corrosion. Whereas geopolymer exhibits sufficient mechanical strength as a binder and it facilitates recycling of waste materials such as fly ash. Moreover, it exhibits higher resistance against fire, acid, and sulfate (Hardjito et al., 2004; Majidi, 2009; Mallikarjuna et al., 2019).

Based on the mentioned approach, some researchers used geopolymers as a binding agent for the RE structures. For example, Cristelo et al. (Cristelo et al., 2012) evaluated the effectiveness of alkaline activation of fly ash for stabilizing soil for RE structures. They investigated the effect of different parameters including the concentration of alkaline activators, liquid to solid ratio, the addition of calcium hydroxide, superplasticizer, and sodium chloride on the compressive strength of samples. Maskell et al. (Maskell et al., 2014) investigated the application of geopolymer for RE stabilization to evaluate if this method enhances water resilience. Sodium silicate and sodium hydroxide were chosen as activator in different mix designs. The compressive strength of samples was measured in both dry and saturated states. They found sodium silicate as the most effective activator for improving strength. Their work exhibited the potential of geopolymers for improving the strength of RE.

In another study, Sore et al. (Sore et al., 2018) stabilized compressed earth blocks (CEB) using geopolymer and compared their performance with cement-stabilized and non-stabilized-CEBs. They made geopolymer-stabilized samples with different percentages of geopolymer contained metakaolin and 12 M sodium hydroxide. They measured the physical characteristics, mechanical properties (wet and dry compressive strength, three-point flexural strength), and thermal properties of CEBs. Their experiments exhibited a noticeable enhancement in the mechanical properties of geopolymer-stabilized samples. Additionally, no significant change was detected between the

thermal characteristics of geopolymer-stabilized and non-stabilized-CEBs. In one recent study, Preethi and Reddy (Preethi and Reddy, 2020) conducted an experimental study on geopolymers to be used in compressed earth bricks. They used a ground granulated blast furnace (GGBS) and fly ash with alkaline activators in different molarities to stabilize specimens with geopolymer. They applied wet compression strength as an indicator of strength improvement. The effect of different concentrations of alkali activators, various proportions of fly ash and GGBS and clay content were assessed. It was concluded that the addition of GGBS and fly ash to the samples will improve their strength. Also, leaching of salt in the geopolymerized samples caused efflorescence which had no influence on the strength of the bricks.

2.1.3.2 Clay and rammed earth

Clay acts as a key element for RE structures and it is used as a binder especially for unstabilized RE (Ciancio and Beckett, 2015). The role of clay content on the engineering properties of unstabilized RE has been investigated and a value of 5 to 20% was suggested (Liu and Tong, 2017). Also, the clay content should be in a certain range for the stabilized RE, for example, at least 20 to 35% of fine particles (i.e. clay) is suggested in the literature (Maniatidis and Walker 2008; Bui et al., 2013; Siddiqua and Barreto, 2018).

Clay structure

The clays are created from the weathering effect on the rocks and their particle size is less than sand and silt (< 2μm). Different clay minerals can be formed based on multiple factors including topography, climate, vegetation, and time. The clay particle is defined as a mineral core with a negative charge encircled by positively charged cations that leave the mineral neutralized. (Nelson et al., 2015). Clays mostly contain crystalline structures of silicates and aluminum. They are formed by the combination of tetrahedral or octahedral units (Bergaya et al., 2013). The most

common clay minerals that are formed based on a different combination of crystalline units are as follows: kaolinites, montmorillonites, illites, and chlorites.

The kaolinites are formed by an aluminum octahedral layer that is positioned on the top layer of tetrahedral units with the chemical formula of $Si_4Al_4O_{10}(OH)_8$. The force that attracts these units is due to the oxygen bond from the tetrahedral unit with the hydroxyl from the octahedral unit which is strong enough against water to penetrate (Bergaya et al., 2013). The montmorillonite structure is a 2:1 structure in which two tetrahedral units are on the top and bottom of one aluminum octahedral unit. The chemical formula of the montmorillonites is $Al_4Si_8O_{20}(OH)_{4n}H_{20}$. This type of clay mineral is mostly penetrable by water because of the weak bonds between its structural unit layers that cause soil expansion (de Carvalho et al., 2015). The illite structure has one aluminum octahedral unit between two tetrahedral units similar to montmorillonites and it is a less expansive mineral. This is caused by the stronger bonds between the structural units due to the interchangeable ions of potassium that prevent water absorption. The chlorite group has a 2:1 structure including one octahedral sheet between two tetrahedral units and a brucite layer between each 2:1 structure (Bergaya et al., 2013).

Bentonite as a stabilizer

A mine located in Kamloops, British Columbia, Canada is estimated to have about 30 million tonnes of raw Ca-bentonite. The possibility of utilizing this material as a binding agent for different construction applications such as RE is barely investigated. Bentonite mainly consists of smectite mineral group that mostly contains montmorillonite. The fine aluminosilicate particles in bentonite are making it a possible additive for stabilizing soil (Hu et al., 2009). Two types of bentonite are calcium bentonite (Ca-bentonite) and sodium bentonite (Na-bentonite). The ion exchangers in

these two types are Na^+ and Ca^+, respectively. The Na^+ ions have a higher attraction to absorb water and this makes the Na-bentonite high swelling bentonite (Siddiqua et al., 2011; Siddiqua et al., 2014). On the contrary, the Ca^+ ions have less tendency for water absorption and consequently low swelling characteristics which makes the Ca-bentonite a proper candidate for RE stabilization technics.

The main elements of Ca-bentonite are including silica, alumina, and calcium have pozzolanic properties which can also be found in the PC and fly ash with different quantities (Dananaj et al., 2005). To the best of author knowledge, no study has been performed on evaluating Ca-bentonite as a stabilizer in RE structures. However, there are multiple studies conducted to evaluate its properties as a proper binding agent. The effect of bentonite on sand stabilization and lime was studied by Wayal et al. (Wayal et al., 2012). They measured the compressive strength of different mixtures and found the optimum 15% bentonite for UCS improvement. They concluded that the improvement in mechanical properties is caused by bentonite that enhances the cohesive bonds between the soil particles.

3 Chapter 3: Methodology

3.1 Overview

The overall goal of this research is to develop and assess innovative waste-to-product technologies and strategies for the transformation and effective utilization of pulp mill residues in the construction sector. To attain this goal, separate laboratory experiments were performed on RE samples with different mix designs to evaluate their performances. This chapter explains the materials and methods for the characterization of materials, mix proportions, and alkali-silicate activator solutions that were used to make samples. Further, it presents a brief description of physical, mechanical, and durability tests that were performed on RE samples.

3.2 Material selection

The natural soil used in this study was collected from a local construction site in Kelowna, British Columbia (BC). This natural soil was used to develop a well-graded model soil with the intended amount of course and fine aggregates using the following steps in the laboratory. Initially, the oven-dried soil was passed through sieve #10 (2 mm size) to separate the coarse fractions and fine fractions (Muhammad and Siddiqua, 2019). Later, the coarse fraction was removed and the remaining fine fraction (less than 2 mm) was passed through sieve #40 (425 μm size). The

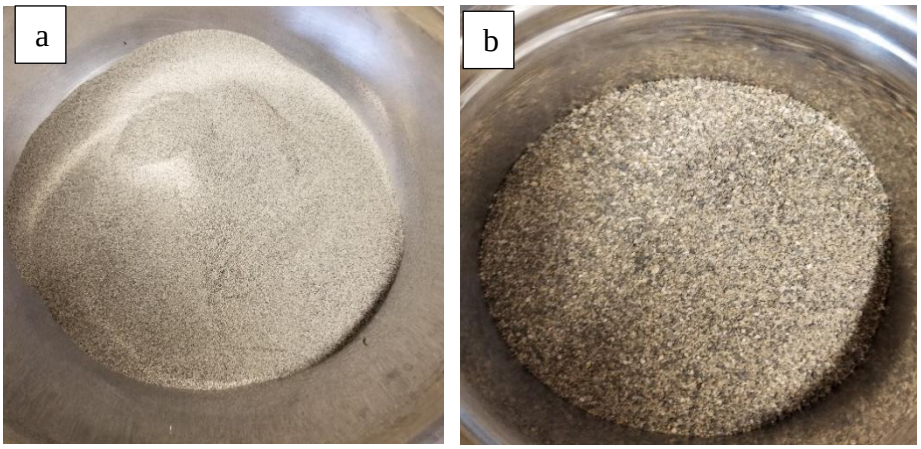

Figure 3.1 (a) The fine fraction, and (b) the coarse fraction of the soil.

composition of new model soil consisting of coarse aggregates (retained on 425 µm sieve) and fine aggregates (passing through 425 µm sieve) in a 2:1 ratio was used to prepare all RE samples (Figure 3.1).

The PFA sample was collected from a local Kraft pulp mill in Kamloops, BC, Canada (Figure 3.2) and its physico-chemical, mineralogical, and morphological characterization, as well as environmental impact, was identified. The Portland cement, which was required for preparing the control RE samples (with 10% PC) and other design mixtures with different combinations of PC, PFA, and activator solutions was locally purchased from a hardware store. The calcium bentonite was supplied in a dry powder form by Pacific Bentonite Ltd., a local mine from Kamloops, BC (Figure 3.3).

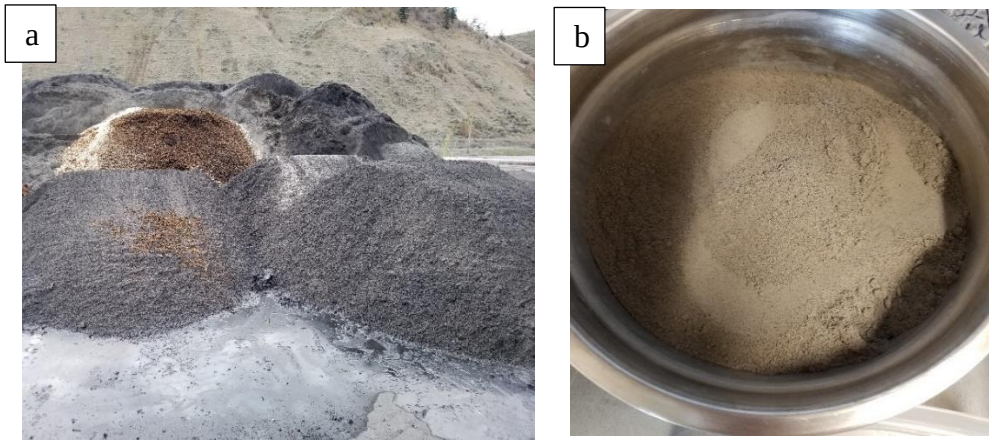

Figure 3.2 (a) The PFA dumped at the pulp mill (b) The PFA powder at the laboratory.

Figure 3.3 The Ca- bentonite.

A sodium-based activator solution, using sodium silicate (Na_2SiO_3) as a supplementary silicate source and sodium hydroxide (NaOH) as the alkali source, was prepared to synthesize the PFA-based geopolymer. These chemicals can facilitate the enhanced reactivity of PFA by the sequential dissolution of alumino-silicate bonds in amorphous fly ash particles. This is due to alkali attack followed by polymerization and growth of amorphous three-dimensional alumino-silicate compound that in turn binds the soil aggregates and improve the strength of RE material (Leong et al., 2018). The physical and chemical properties of these binders are listed in Table 3.1. The different proportions of activator solutions were derived based on the relevant literature (Hardjito and Rangan, 2005; Cristello et al., 2012b; Leong et al., 2018). The three alkali concentrations of

8M, 10M, and 12M NaOH were used in a 1:2 ratio with Na_2SiO_3, and the activator solution was added to the ash in a 2:1 ratio (Figure 3.4).

Table 3.1 Characteristics of chemical binders.

Properties	Sodium hydroxide	Sodium silicate
State	Solid	Liquid
pH	14	11.2
Relative density	2.13	1.4
Molecular weight	40	-
Chemical Composition	NaOH	Na_2SiO_3

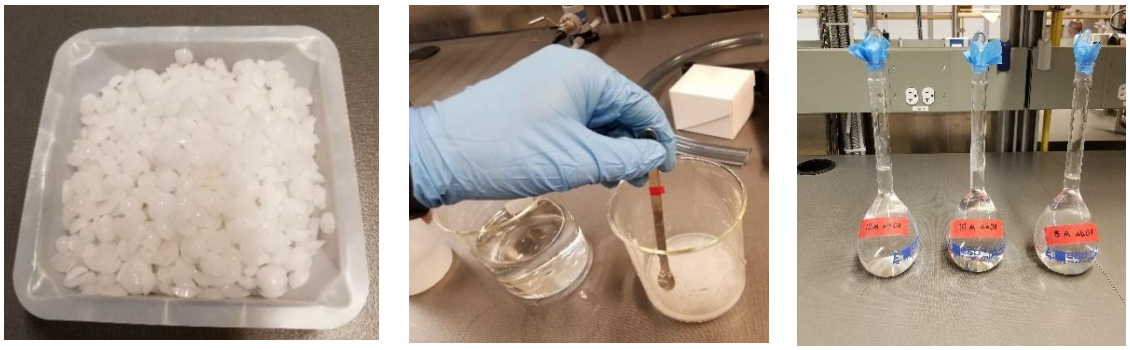

Figure 3.4 Preparation of NaOH solutions.

3.3 Formulation of rammed earth mix designs

Table 3.2 describes the summary of mixed designs. In this study, two batches of samples were prepared. The first batch of samples was treated with a mix of soil, PFA, cement, and the alkali-silicate activators. In the second batch, samples were treated using soil, cement, Ca-bentonite, and PFA without any alkali-silicate activators. The optimum moisture content (OMC) and maximum dry density (MDD) for the different RE design mixes were determined based on the miniature Proctor compaction method (Sridharan and Sivapullaiah 2005). To make the different soil-binder mixtures, the dry components such as the model soil aggregates, powdered PFA, Ca-bentonite, and PC were initially hand-mixed for 10 to 15 minutes.

For the first batch, the control RE specimens were prepared using 10% PC as a binder (denoted as SC). The feasibility of using a PFA-geopolymer as a replacement for PC was assessed in terms of using: (i) 10% PFA (denoted as SP) and (ii) 5% PC + 5% PFA (denoted as SCP55). The NaOH solutions of different molarities (8M, 10M, and 12M) were prepared by dissolving the required amounts of dry pellets in RO water and continuously stirring for 10 minutes. Further, the NaOH solution was allowed to cool down, and Na_2SiO_3 (in liquid form) was added to this solution to provide enough silica source for the complete mobilization of the geopolymerization process (Majidi, 2009; Cristelo et al., 2012a; Muhammad et al., 2018). In the next stage, the activator solution was added to the prepared dry mixture in a 2:1 activator to ash ratio and an additional amount of deionized water was added to achieve the corresponding OMC.

For the second batch, all samples contained 5% cement and 15% Ca-bentonite, and their PFA content varied between 5% PFA (denoted as SCPB5515), 10% PFA (denoted as SCPB51015), and 20% PFA (denoted as SCPB52015). To evaluate the effectiveness of PFA itself and comparing with the influence of Ca-bentonite, two more samples containing 10% PFA (denoted as SCP 510), and 20% PFA (denoted as SCP520) were prepared.

Table 3.2 Summary of test methods.

Mix Mode	Alkali-silicate activation Solution		The mass ratio of material to 1 kg				Curing design	
	NaOH concentration (Molarity)	($NaOH/Na_2SiO_3$ ratio)	Soil	PFA	PC	Ca-bentonite	Curing temperature	Curing days
SC	-	-	0.9	-	0.1	-	Ambient (~22°C)	7, 28
SP	-	-	0.9	0.1	-	-	”	”
SCP55	-	-	0.9	0.05	0.05	-	”	”
SCP55-8M	8	1:2	0.9	0.05	0.05	-	”	”
SCP55-10M	10	1:2	0.9	0.05	0.05	-	”	”
SCP55-12M	12	1:2	0.9	0.05	0.05	-	”	”
SCPB5515	-	-	0.75	0.05	0.05	0.15	”	”
SCPB51015	-	-	0.7	0.1	0.05	0.15	”	”
SCPB52015	-	-	0.6	0.2	0.05	0.15	”	”
SCP510	-	-	0.85	0.1	0.05	-	”	”
SCP520	-	-	0.75	0.2	0.05	-	”	”

3.4 Material characterization

3.4.1 Specific gravity

Soil: The specific gravity is defined as the ratio of soil aggregate mass to the mass of water with an equivalent volume of aggregates. The value of specific gravity is usually used to determine the volume of the aggregate for being used in different mixes. The ASTM C128-15 (ASTM C128, 2015) guideline was employed for the determination of the specific gravity. At first, the oven-dried soil samples were immersed in the water for 24 hours. The excess water was removed and the soil was spread on a surface while warm air was slowly blowing on that. The purpose of this was to have the soil in a saturated surface dry condition. After reaching that state, the mass of 500 grams of saturated surface dried soil was introduced in a pycnometer filled with RO water. After agitating the pycnometer for releasing the air bubbles, it was filled with water at a standard temperature and the mass of the pycnometer with the soil and water was recorded. Then the mass of the soil was oven-dried for 24 hours and the mass was measured as well. Further, the mass of the pycnometer filled with water was noted at a standard temperature. After measuring all the required masses, the specific gravity of the soil was measured based on the following equation, specific gravity = A/ (B+S-C), where A is the mass of the oven-dried specimen, B is the mass of pycnometer filled with water, S is the mass of saturated surface dry soil, and C is the mass of pycnometer filled with water and soil.

Pulp mill fly ash: The specific gravity was measured using the water pycnometer method (ASTM D854, 2014). At first, the weight of the dry pycnometer and 500 ml pycnometer filled with a de-aired RO water was measured. The temperature of the water was noted as well. Afterward, 50g of dried PFA was poured into the pycnometer and the de-aired RO water was added into the pycnometer and it was shaken until PFA was fully dissolved. Subsequently, more water was

poured into the pycnometer to reach the specified level. The temperature and the mass of the pycnometer with PFA and water were measured. Then the solution of water and PFA was poured into a becker and the PFA was segregated from the water by a filter paper. The weight of the PFA was quantified after 24 hours of oven drying.

3.4.2 Particle size distribution

Soil: The particle size distribution (PSD) was determined using standard dry sieve analysis (ASTM D2487-17, 2017). This method classifies soils using a standard system and identifies three categories of coarse-grained soils (more than 50% of the soil particles remain on sieve No.200), fine-grained soils (50% or more of soil particles passing the sieve No.200), and highly organic soils. In this method, a stack of sieves (Figure 3.5) was employed from the top to bottom in the following order of 3/4", 3/8", No.4, No.10, No.20, No.40, No.60, No.140, and No.200. About 500g of dried soil was passed through the stack using a mechanical shaker for at least 10 minutes. The mass ratio of the fraction of the retained soil of each sieve over the whole amount of the soil represents the percentage of each particle size range on the PSD curve. Based on this classification, it calculates the coefficient of uniformity, C_u, and the coefficient curvature, C_c, as follows: $C_u = D_{60}/D_{10}$ and $C_c = D_{30}^2/D_{10}*D_{60}$, where D_{10}, D_{30}, and D_{60} are the particle size diameters that 10, 30, and 60% of the soil particles are smaller than those diameters.

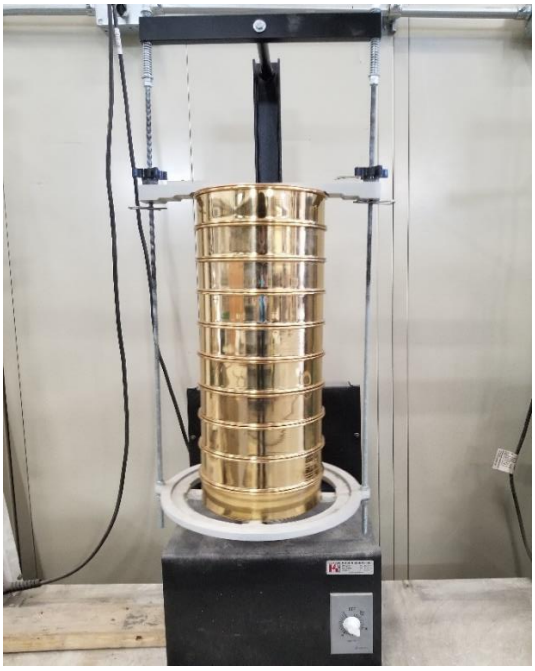

Figure 3.5 Stack of sieves in the mechanical shaker.

Pulp mill fly ash: The PSD of the PFA was achieved through the hydrometer test method based on the ASTM D7928-16 (ASTM D7928-16, 2016). First, 50g of PFA fine particles that were passed through 75µm (No.200) sieve, were immersed in a 125 ml of sodium hexametaphosphate solution (with the concentration of 40g in 1000 ml RO water) for 16 hours. After that, the solution was poured into a blender and mixed for 1 minute at the rate of 10,000 rpm. The blended solution was poured into a 1000 ml cylinder (Figure 3.6). The cylinder was shaken back and forth for 1 minute. Two other cylinders were chosen as well, one of them was filled with RO water and the other one was the control solution that was filled with 125 ml of sodium hexametaphosphate (the concentration of 40 g in 1000 ml) and RO water until the 1000 ml mark. The hydrometer readings of the solution cylinder started after 2, 4, 8, 16, 30, 60, 120, 240, and 1440 minutes from shaking the solution. The process of the hydrometer test is based on the fact that particles with different diameters settle at different times. For the correction factor, temperature and hydrometer readings from the control cylinder and the RO water cylinder was determined at the same time intervals.

The hydrometer test results were used to draw the PSD graph for the particle diameters less than 75µm. For the portion of PFA retained on sieve No.200, the sieve analysis was performed and the final PSD graph was driven.

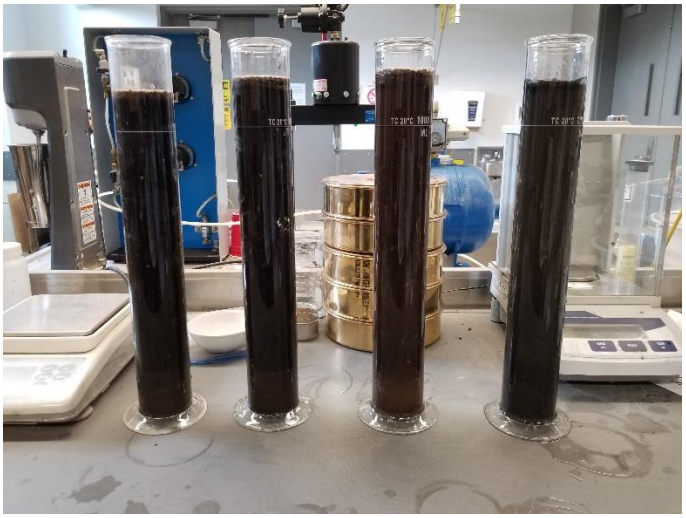

Figure 3.6 Slurry blend of PFA in 1000 ml cylinder.

3.4.3 Laser diffraction method

The PFA and Ca-bentonite particle size analysis were evaluated by the laser diffraction method as well. This method is based on the interaction between the particle size and the light as a specific particle size scatters the light by a certain angle. A laser beam passes through a cell that contains the suspended sample and the diffracted light is captured by a detector (Loizeau et al., 1994). The powder samples were dried and passed through the sieve No.200. The test was performed by Malvern Mastersizer 3000 device (Figure 3.7).

Figure 3.7 The laser diffraction test device

3.4.4 Natural moisture content of the pulp mill fly ash

The natural moisture content (NMC) of PFA was measured as per ASTM D2216-19 (ASTM-D-2216-19, 2019). The mass of three PFA samples was measured initially. Based on the table provided in the standard, the mass quantity is related to the size of the sample. Then, the samples were dried in the oven for 24 hours at 110 °C. The moisture content was determined based on the loss of mass (mass of water) over the mass of dry specimens.

3.4.5 pH of pulp mill fly ash

The pH of PFA was measured as per ASTM D4972-19 (ASTM D4972, 2019) guidelines using a Thermo Scientific Orion 5 Star pH meter. A 10 g of oven dried PFA was mixed with 50 ml RO water and the solution was vibrated for proper mixing of PFA and water. The solution pH was determined after 1 hour by using the pH meter.

3.4.6 Loss on ignition of pulp mill fly ash

Total carbon (TC) content was determined based on the loss-on-ignition (LOI) method as per ASTM D2974-20 (ASTM D2974-20e1, 2020). This test is quantifying the amount of unburned carbon in the PFA. The increase in LOI indicates that there are higher carbon content, which

decreases the quality of fly ash (Bhatt et al., 2019). First, the container was placed in the oven at 750 °C for 1 hour. After being cooled in a desiccator (Figure 3.8a) the weight was captured. A 5 g oven-dried PFA was placed in the container and put in the oven at 950 °C for 2 hours (Figure 3.8.b). The sample was placed in a desiccator to cool down and the weight was captured.

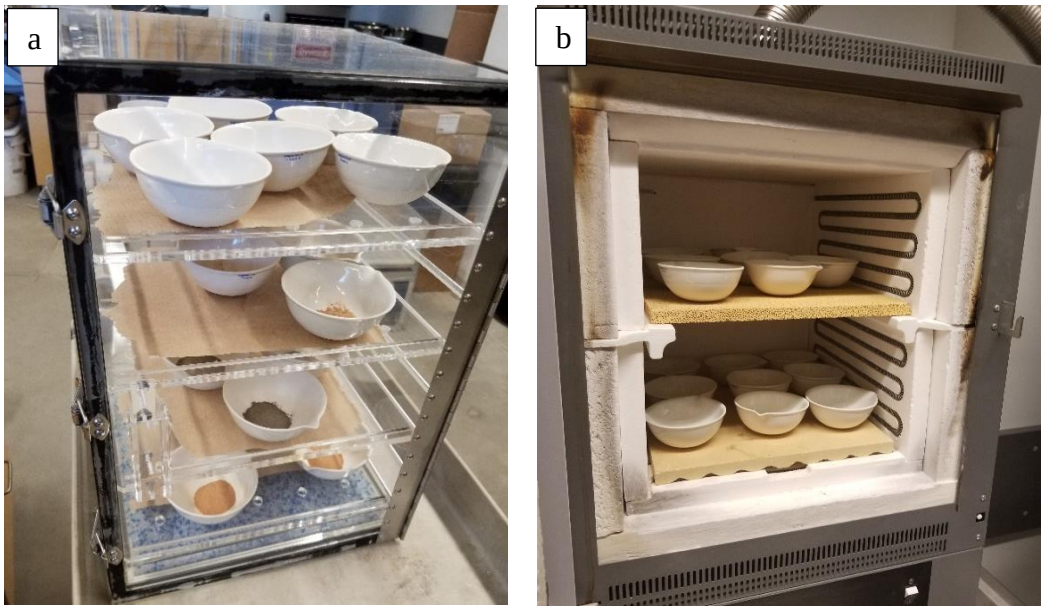

Figure 3.8 Samples for the LOI test at (a) desiccator and (b) oven.

3.4.7 Environmental risk assessment of pulp mill fly ash

Although PFA is generally treated as a non-hazardous industrial by-product, it is essential to perform a source-specific environmental risk assessment since the fly ash chemistry varies with the type of combusted wood species and the nature of combustion processes. The influence of PFA on the environment can be represented based on the amount of its toxicity through its trace metal concentrations. The environmental protection agency (EPA) recommends that the environmental risk of waste materials such as PFA should be assessed regularly in case of using it as a geomaterial in different applications. Toxic trace elements present in the PFA, are categorized in two sections in different studies. First, the elements that risk human health (such as As, Cr, Hg, Pb, and Cd) and

the elements that endanger the plant growth (including Cu, B, Ni, and Zn) (Cherian and Siddiqua, 2019).

The trace element assessment was performed by acid digestion of the oven-dried PFA in aqua-regia (concentrated HNO_3 and HCl in 1:3 ratio) at a high temperature. The digested samples were later cooled down and an aliquot of clear suspensions were diluted for analysis. Agilent 8900 Triple Quadrupole ICP-MS (inductively coupled plasma-mass spectrometry) equipped with a CETAC ASX520 autosampler was used for major, minor, and trace element analysis (Figure 3.9).

Figure 3.9 The ICP-MS setup

3.4.8 Plasticity index of calcium bentonite

The plasticity index is described as the difference value between the liquid limit of soil and its plastic limit. The liquid limit of the soil is defined as the state in which the soil changes from the plastic state to the viscous state. The plastic limit of the soil is defined as the state that the soil behavior is changed from a semi-solid state to a plastic state. All the tests were performed based on ASTM 4318-17. For all the tests, the specimens passed through No.40 sieve. For the liquid limit test, the sample was completely mixed with distilled water until it formed a uniform paste. The paste was then placed on the cup of liquid limit device. Then, a groove was made using a

grooving tool from the highest part to the lowest part from the rim of the cup. The device handle was rotated to produce blows until the two halves of the sample attached at the bottom of the groove. The number of blows and the water content of the sample was recorded. The procedure was repeated for five different water contents and a graph was captured using these points. The liquid limit of the sample was the water content with 25 blows required. For the plastic limit, the same procedure that was used for the liquid limit was employed. About 20 g of the prepared sample paste was spread on a glass surface to reduce its water content. Then the paste was rolled between the palm and the glass plate until its diameter reached 3.2 mm. The process was repeated until the thread started to crumble and the sample could not be re-rolled to a thread in 3.2 mm diameter. This procedure was repeated five times and the moisture content of the sample was captured after each time. The average moisture content was considered as the plastic limit of the sample.

3.4.9 Swelling index test of calcium bentonite

The swelling index test was carried out based on ASTM D5890-19 (ASTM D5890 − 19, 2019). About 2 g of the oven-dried Ca-bentonite was used in this test. The cylinder was filled with 90 mL of reagent water. About 0.1 g increment of the bentonite was added to the cylinder and it was allowed to settle at the bottom of the cylinder for 10 minutes before the next increment was poured. After the entire 2 g of the bentonite was added, the cylinder was covered with a lid for 16 hours to let the clay settle and hydrate. After that, the volume level at the top of the settled bentonite was noted. Later, by using a thermometer the temperature of the mixture was recorded as well.

3.4.10 X-ray diffraction analysis

The X-ray diffraction analysis (XRD) analysis was performed to determine the chemical-mineralogical composition of PFA and Ca-bentonite. This method is an effective tool to analyze the mineralogy and crystallization of samples. It is based on interacting X-ray waves with the

charges of electrons in atoms. This interaction will cause the emission of the spherical wave. The amplitude of the emitted wave is measured to recognize different elements. The X-ray wave of each molecular bond has a specific pattern. A mixture containing various elements will produce a reflected X-ray pattern comprising all the individual elements present in the mixture. A database of multiple patterns from different components is employed to identify various elements of a mixture (Stanjek, 2004).

The X-ray tests were conducted in the Department of Earth, Ocean, and Atmospheric Sciences at the University of British Columbia, Vancouver, BC. The samples sent for testing were dried at the oven and were ground to the optimum grain-size range less than 10 μm for quantitative X-ray analysis by grinding in a vibratory McCrone Micronizing Mill for 7 minutes. Then, samples were mounted in standard back mount holders. Continuous-scan X-ray powder-diffraction data were collected over a range of 3-80°2θ with $Co K\alpha$ radiation on a Bruker D8 Advance Bragg-Brentano diffractometer.

3.4.11 Morphological analysis

The morphology and composition of PFA, cement, Ca-bentonite, were obtained through SEM-EDS analysis with the aid of Tescan Mira 3 XMU SEM instrument coupled with Oxford Aztec X-max EDS detector (Figure 3.10a). The samples were captured from the middle part of oven-dried samples and passed through sieve No. 200. Then, they were coated by palladium and platinum at a ratio of 20/80 in a high vacuum argon atmosphere (Figure 3.10b) and placed inside the instrument for the analysis.

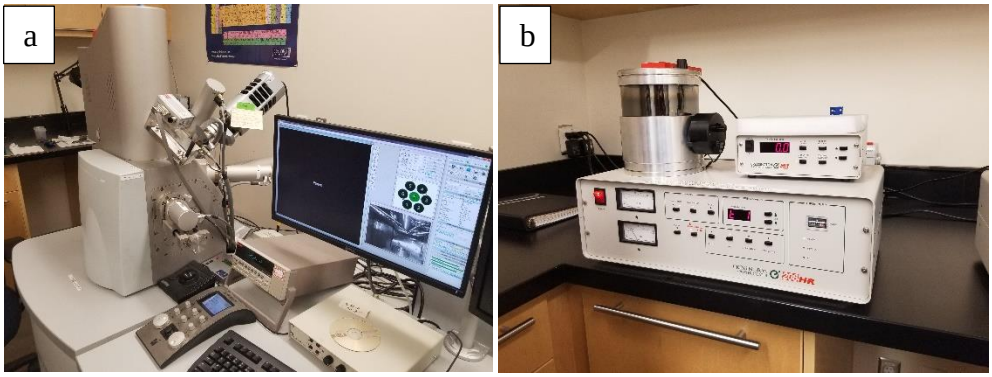

Figure 3.10 (a)The SEM and EDS setup (b) The sputter coater for coating the powdered samples

3.4.12 Compaction characteristics

The compaction test was carried out to obtain the graph of maximum dry density (MDD) versus the optimum moisture content (OMC) of different mixed designs based on the miniature Proctor compaction method (Sridharan and Sivapullaiah, 2005). The required quantity of oven-dried materials was completely mixed, and the targeted moisture content was added to the mixture. To certify the water is properly distributed in the sample, it was stored in air-tight plastic bags for 16 hours. Then, samples were compacted into three layers with the standard compaction energy in the mold (Figure 3.11). The mass of compacted soil sample was obtained to calculate the dry density. The water content of each sample was determined as well. At least five points were identified for each sample to provide the compaction curve.

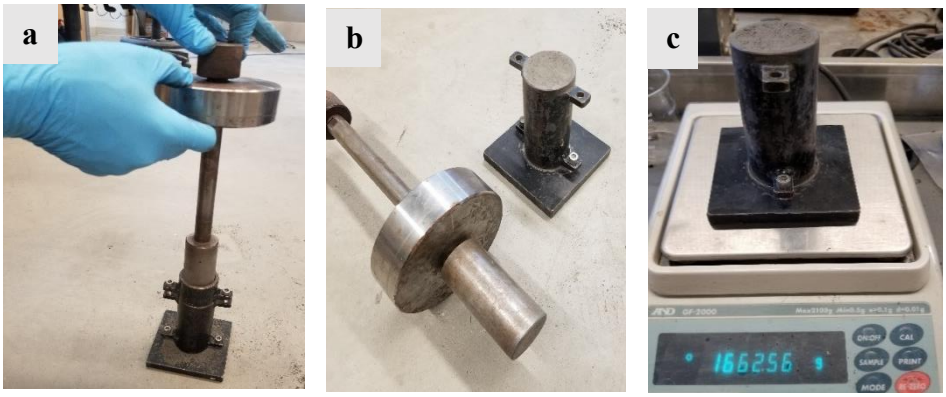

Figure 3.11 The procedures for assessing the compaction characteristics of mixed designs. (a) compacting the soil sample (b) the hammer and the mold (c) Measuring the mass of the compacted sample.

3.5 Sample preparation and curing for strength and durability tests

Each sample was compacted in three layers to reach their MDD in a 38 diameter × 76 mm high PVC split mold fabricated at the in-house workshop facility (Figure 3.12). The specimens were kept in a moist room with 80% relative humidity and an ambient temperature of 22 °C for 7 days and 28 days of curing. After curing, specimens were extruded from the PVC molds and tested for compressive strength and weather durability tests. At least three samples were prepared for each mix design while conducting UCS and freeze-thaw durability tests to ensure the reliability and repeatability of the obtained results.

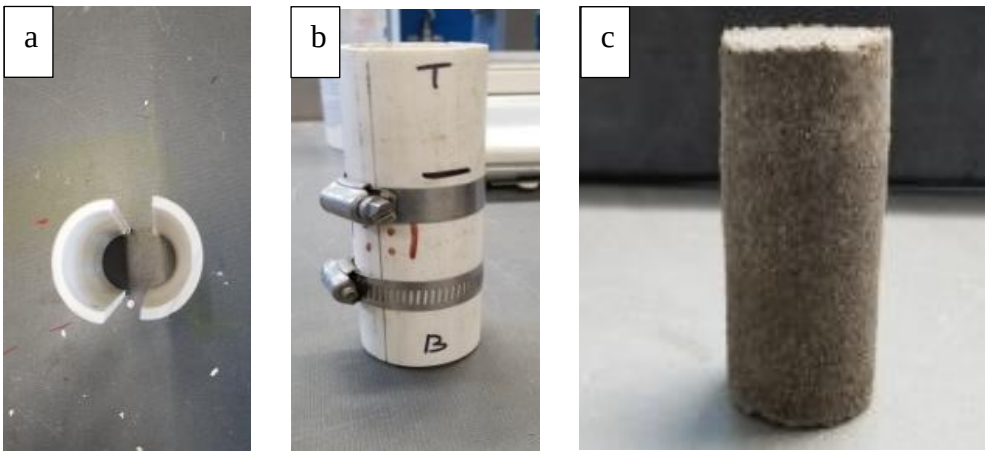

Figure 3.12 illustrations of samples. (a,b) PV C split mold, (c) cured specimen.

3.5.1 Uniaxial compressive strength test

Pulp mill fly ash: The unconfined compressive strength (UCS) were determined as per the, ASTM D4219-08. For UCS determination, the cylindrical PFA specimens with dimensions of 36×72 mm were prepared and cured for 1 day in the moist room with 80% humidity and ambient temperature (~22 °C). The cured specimens were tested using a uniaxial compression testing machine at a strain rate of 1% per minute and stress-strain characteristics were recorded to calculate the UCS value.

Mix design: As the samples were prepared and cured based on the method described above, the UCS test was carried out according to ASTM D4219-08, and the vertical loading rate was fixed at 0.78 mm/min to the failure point of the samples. For each set of samples, at least three tests were performed (Figure 3.13).

Figure 3.13 The UCS test setup.

3.5.2 Freeze-thaw durability test

Since the continuous freezing and thawing cycles cause the deterioration of structures, the freeze-thaw durability tests were performed to evaluate the functionality of the mix designs in the cold weather. The test was conducted based on ASTM D560-12 (D560-12, 2012) guidelines. After preparing the mixed designs explained in the previous section, they were cured for 28 days. Based on this standard, compacted RE samples were cured and subjected to 12 alternate freezing and thawing cycles (freezing at -23 °C in a chest freezer for 24 hours and thawing in the moist room at +22 °C temperature). The sample replicates (at least three replicates for each set) were tested after completing 6, and 12 cycles to determine the trend in UCS variation as the indicator of frost

resilience (Lake et al., 2017). Also, before and after each stage of the freezing and thawing cycle, the weight, dimension, and moisture content of each specimen were recorded.

3.5.3 Molecular characterization of stabilized rammed earth using Fourier transform infrared

The Fourier transform infrared (FTIR) is a method to collect the transmitted infrared (IR) spectrum of a sample. When the IR radiation passing through the sample, part of it will be absorbed and the rest will be reflected. Since different chemical structures absorb and transmit the IR in their specific spectrum, the final transmitted signal from a sample is a spectrum that represents the molecular structures. The FTIR method was carried out on the first set of samples in different curing times to evaluate changes in the molecular structures. The IR spectra were recorded using the reflectance geometry in the mid infra-red, MIR, region (400 to 4000 cm^{-1}) with a resolution of 4 cm^{-1} with the aid of Shimadzu IR Prestige-21 instrument equipped with Attenuated Total Reflection (ATR) module (Figure 3.14).

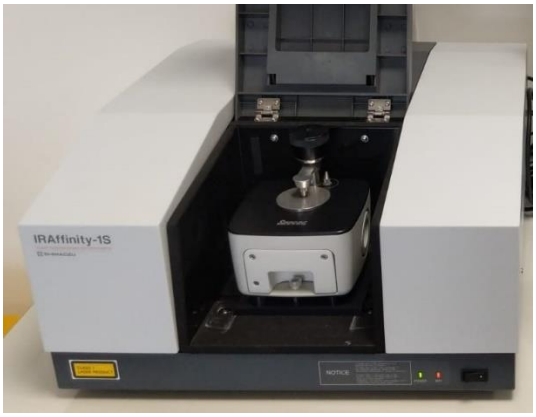

Figure 3.14 The FTIR instrument.

3.5.4 Microstructural analysis using SEM-EDS

The advanced characterization of stabilized RE was carried out using SEM-EDS analysis to evaluate the reaction mechanisms and micro-level changes that caused strength and durability improvement of rammed earth.

3.5.5 Leachate analysis using ICP-MS

To evaluate any possible contaminations that were sourced from the hazardous heavy metals that are leached from the PFA, the environmental risk assessment was conducted. This test was performed on the PFA, Ca-bentonite, PC, the control sample, and the optimum PFA-treated samples, based on the water batch extraction method as per the Canadian council of resource and environment ministers (CCREM, 1987) guidelines. Initially, the samples were powdered and mixed with deionized water in the liquid-to-solid ratio of 5:1. Subsequently, the solutions were placed on an orbital shaker for 48 hours to be continuously mixed. Then, the mixture was filtered to obtain supernatant liquid and was tested for trace element concentrations using ICP-MS.

Chapter 4: Results and discussion

4.1 Characterization of the soil

The obtained PSD curve of natural soil is illustrated in Figure 4.1. It consists of less than 1% fines (silt + clay fractions), 27% fine sand, 51.7% medium sand, 14.1% coarse sand, and 6.2% gravel. Further, the natural soil was classified as poorly graded sand (SP) as per the unified soil classification system, USCS (ASTM D2487-17e1). The specific gravity of soil was 2.65.

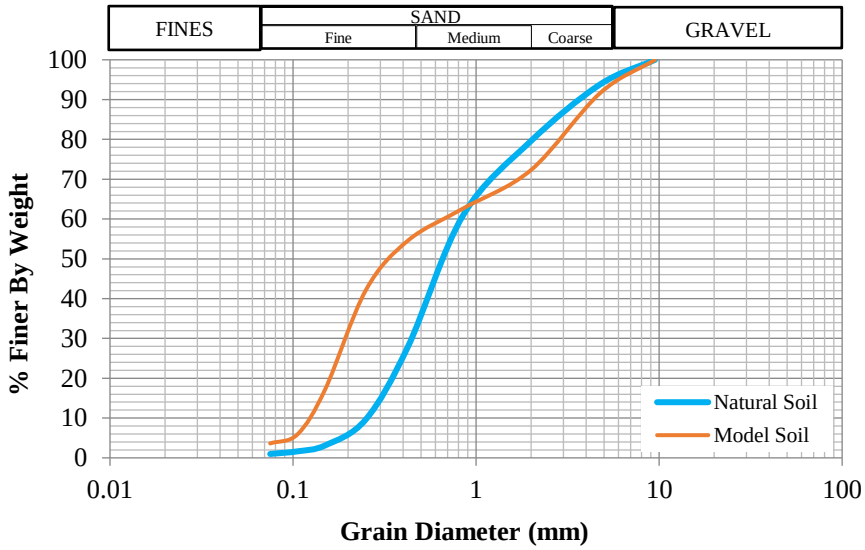

Figure 4.1 Particle size distribution for the natural soil.

4.2 Characterization of PFA

The important physicochemical and mechanical properties of PFA are presented in Table 4.1. As shown in Figure 4.2, the SEM image of PFA showed a heterogeneous mixture of some unevenly formed crystalline and amorphous inorganic ash particles, and few spherical cenospheres were observed (Cherian and Siddiqua 2019). Most of these structures are highly porous and hydrophilic (water absorbent) in nature (Pitman 2006). Also, there are some partially combusted wood particles identified amongst the porous structures.

Table 4.1 Physicochemical and mechanical properties of pulp and paper mill fly ash.

Properties					**Value**
Specific gravity, G					2.87
Natural moisture content, NMC (%)					29.72
Fineness, D_{50} (µm)					16
Maximum dry density, MDD (kN/m^3)					6.53
Optimum moisture content, OMC (%)					38.26
Loss on ignition, LOI (%)					30
pH					12.95
Unconfined compressive strength, UCS (kN/m^2)					675
Elemental composition (%)					
Si	Al	Ca	Fe	K	Mg
12-26	6-8	14-28	4-9	1-7	0.5-3

The results of EDS analysis revealed that the major part of the PFA surface contained oxides of calcium (Ca), silicon (Si), and aluminum (Al) with minor amounts of Mg, Na, K, and Fe oxides. The mechanical and cementitious properties of PFA are significantly influenced by the predominance of calcium, followed by aluminosilicate components (like SiO_2, Al_2O_3, and Fe_2O_3. Moreover, it was confirmed that PFA can be a potentially active aluminosilicate precursor to synthesize geopolymer binders of high mechanical performance.

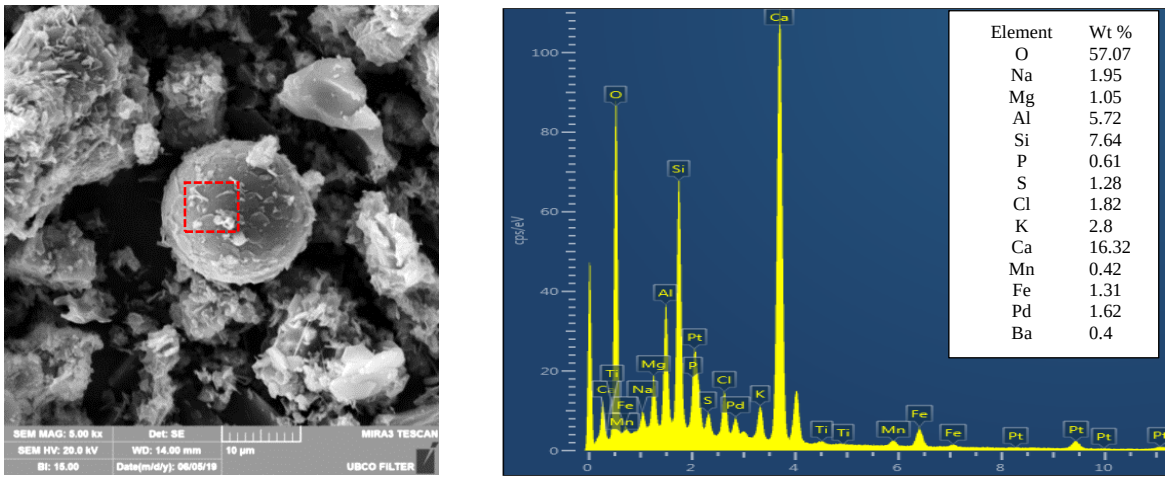

Figure 4.2 SEM and EDS results of PFA.

Based on the Rietveld quantification of X-ray diffractograms (Figure.4.3), the PFA sample mainly constituted 46.4 % calcium silicate, 27.4 % calcite, 18.3 % calcium hydroxide, and 8.0 %

quartz. These observations further confirmed that the presence of a higher amount of calcium and silica compounds in PFA makes it a suitable candidate for binder applications in construction and geotechnical engineering (Cherian and Siddiqua, 2019).

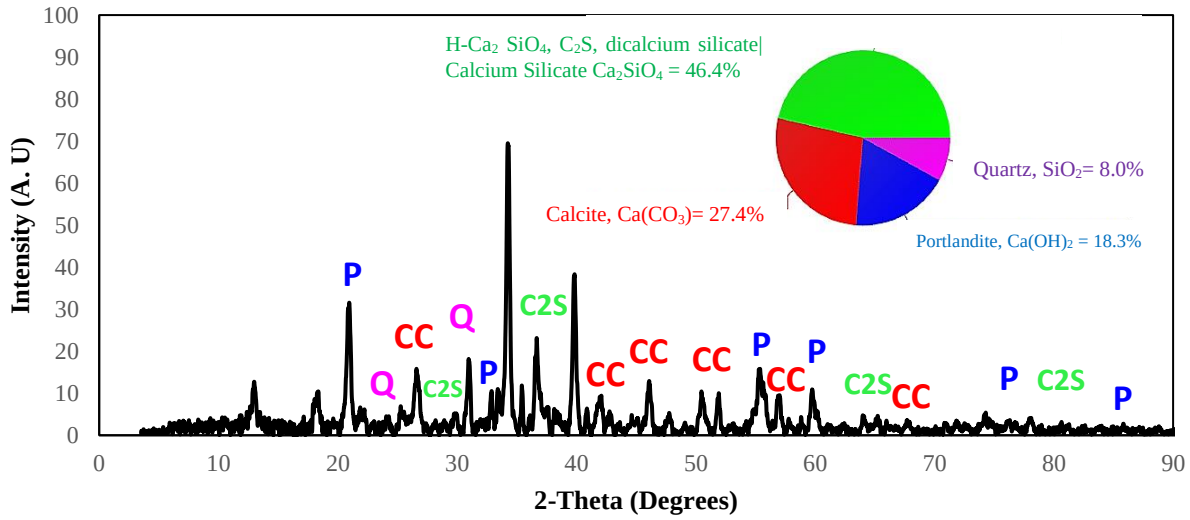

Figure 4.3. X-ray diffractogram of PFA.

Table 4.2 summarizes the results of major, minor, and trace element analysis conducted for PFA. The major and minor metals such as Ca, Si, Al, Fe, Mg, K, Mn, P, etc. have been detected to be more concentrated in PFA than the certified reference material (CRM) which is a coal fly ash.

Table 4.2 Major, minor, and trace element concentrations of pulp and paper mill fly ash based on acid digestion procedure.

	The concentration of major and minor elements (mg/kg)										
	Si	**Al**	**Fe**	**Ca**	**Mg**	**Na**	**K**	**Ti**	**S**	**Mn**	**P**
PFA	31580	13156	11252	6975	13138	2261	39938	553	54351	4477	6668
CRM	27169	15020	5476	3189	2955	17301	19222	1485	36990	209	2397
	Concentration of trace elements (mg/kg)										
	As	**Ba**	**Cd**	**Co**	**Cr**	**Cu**	**Mo**	**Ni**	**Pb**	**Se**	**V**
PFA	19.7	476	3.0	3.5	16.8	67.6	6.1	12.1	56.5	1.32	15.7
CRM	20.4	228	381	5.3	27.7	203	16.5	21.8	5994	1.59	26.3

Furthermore, the heavy metals in fly ash leachate obtained from acid digestion process such as Ba, Pb, Cu, As, V, Cr, have low concentrations when compared to trace levels of Co, Mo, Ni, and

Se. Based on these results, the selected PFA sample can be considered to be environmentally safe for utilization in construction applications without causing any potential dangers.

4.3 Cement specifications

As depicted in Figure 4.4, the SEM-EDS characterization revealed that the particle size and shape of particles as well as the elemental composition was similar to that of PFA. The PC cenosphere exhibited a predominance of calcium oxide followed by a significant amount of silica and a low amount of alumina.

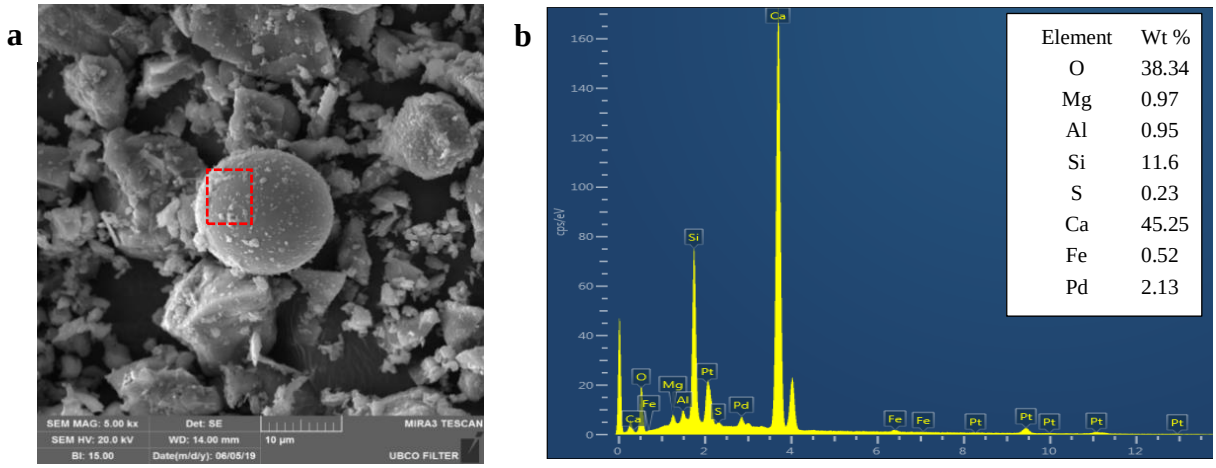

Figure 4.4 SEM and EDS results of Portland cement.

4.4 Bentonite specifications

Various laboratory experiments were carried out to evaluate Ca-bentonite properties. The moisture content was obtained as 4.91%. The PSD properties showed that about 97.2% of the fines passed sieve No.200. The specific gravity was measured as 2.49, and the swelling index was 12 mL/2g;. The liquid limit was 209%, and the plastic limit was about 21%; hence the plasticity index was 188%.

The SEM and EDS analysis (Figure 4.5) revealed that the selected Ca-bentonite has a high silica content. The presence of silica in soil stabilization is necessary to increase the pozzolanic reaction. This specification makes the Ca-bentonite a suitable additive, especially with the PFA having lower silica content. The XRD revealed the chemical components present in the Ca-bentonite was including 41.1% montmorillonite, 53% albite, and 4% quartz.

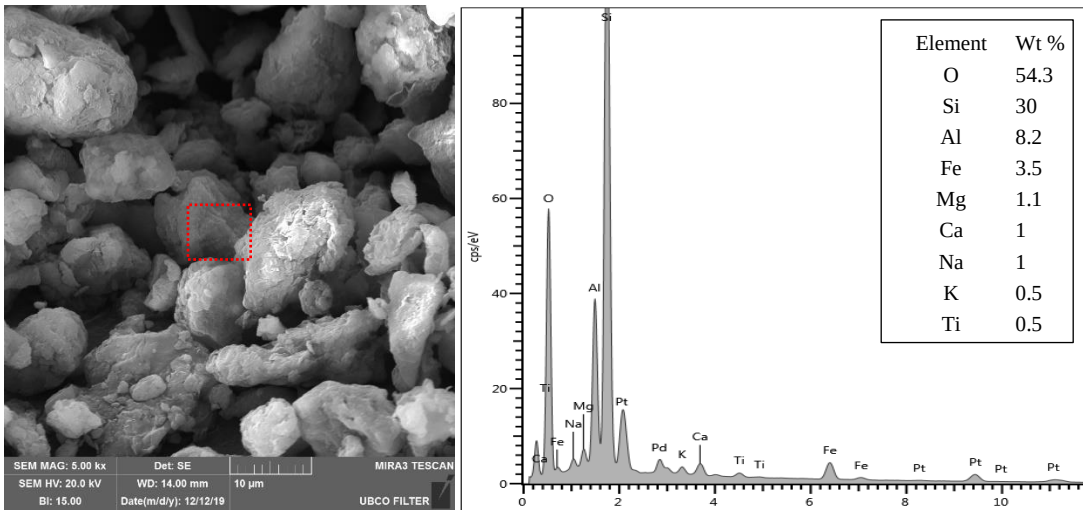

Figure 4.5 SEM and EDS results of calcium bentonite

4.5 Compaction characteristics of rammed earth mixtures

Table 4.3 provides the OMC and MDD of different mix designs. As shown in Figure 4.6, the SC sample had the highest maximum dry density (MDD) and lower OMC when compared to the other two mixtures SP and SCP55. This trend indicated that the addition of PC caused a decrease in the OMC, because of the excess heat generated by the exothermic cement hydration process (Mahvash et al., 2017). On contrary, as it is depicted in Figure 4.7, the increase in PFA content caused an increase in the OMC which is partially associated with extra water required for the hydration reactions and high moisture absorption capacity of PFA particles. The decrease of MDD

with an increase in PFA dosage is also attributed to the dilution of the mixture with relatively lighter PFA when compared to soil aggregates (Makusa, 2013).

Table 4.3 The values of OMC and MDD for different mix designs.

Mix Design	OMC (%)	MDD (kN/m^3)
SC	11	18.16
SP	18.8	17.09
SCP55	17.5	17.52
SCP510	18.86	17.57
SCP520	19.53	14.9
SCPB5515	15.18	18
SCPB51015	18.3	16.89
SCPB52015	24.62	15.13

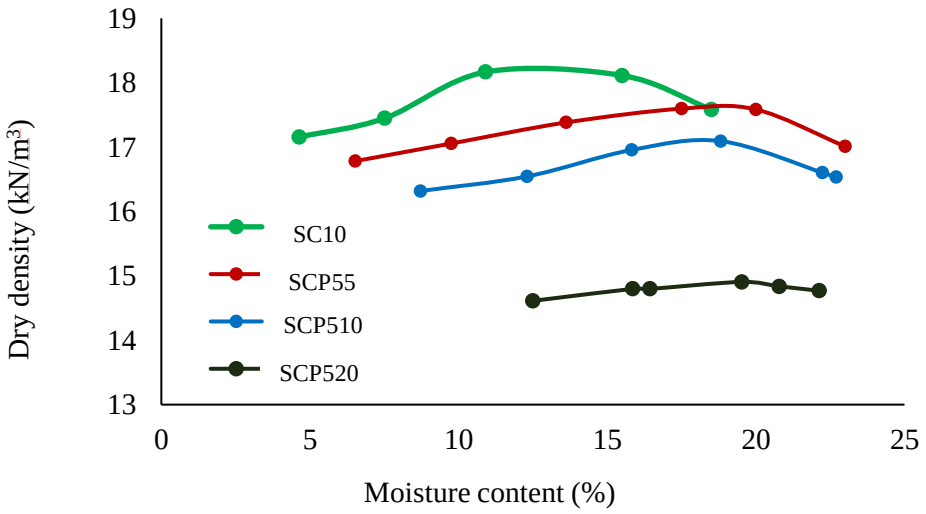

Figure 4.6 The compaction curves of three mix designs.

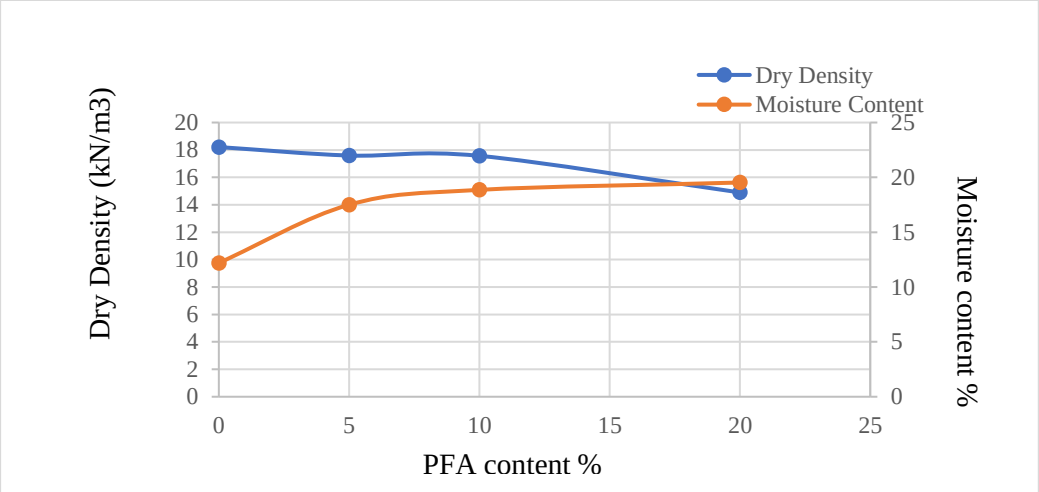

Figure 4.7 The relation between PFA content and OMC and MDD.

4.6 Unconfined compressive strength of rammed earth mixtures

4.6.1 Samples treated with the alkali-silicate activator

Figures 4.8 and 4.9 present the stress-strain characteristics of RE samples treated with different combinations of PC, PFA, and activator solutions, and cured for 7 days and 28 days, respectively. The RE material without activator solution (denoted as SCP55) showed a ductile behavior with very low stiffness properties. Whereas the stabilized material became more brittle by the addition of activator solution, thereby substantially improving the stiffness properties (in the order of SCP55-8M > SCP55-10M > SCP55-12M). Figure 4.10 illustrates the difference in the UCS values of 7-day and 28-day cured RE samples corresponding to different design mixes (error bars represent the standard deviation of the measured values). The 7-day UCS value of SCP55 was reduced to half compared to the control SC specimen (from 1.23 MPa to 0.43 MPa), which indicated that partial replacement of PC with virgin PFA deteriorated the strength of RE material. On contrary, the specimens treated with alkali-silicate activator exhibited significant strength improvement that indicated the effectiveness of alkalinization on the PFA precursor.

The maximum improvement in UCS was achieved for specimens treated with 12M NaOH, up to 4.3 MPa. This phenomenon is probably due to the strengthening of inter-aggregate bonding between soil aggregates by high-performance geopolymer coating. Moreover, the compressive strength of all RE samples increased from 7 days to 28 days indicating that the samples became stronger and stiffer with the time-dependent cementation geopolymerization processes. The highest value of UCS was measured in SCP55-10M specimens (treated with 10M alkali-silicate activator) after 28 days of curing. It is also important to note that the SP samples designed with full replacement of PC with PFA and in the absence of alkali-silicate activator (viz., soil + 10% PFA) could not sustain the compression test after the prescribed curing period.

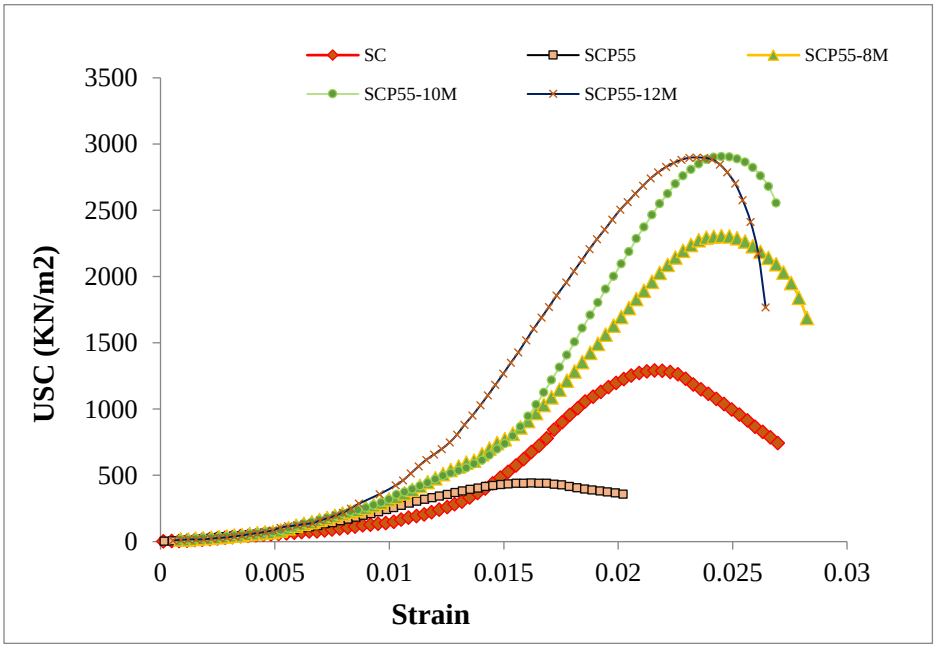

Figure 4.8 Stress-strain characteristics of rammed earth specimens treated with alkali-silicate activator after 7 days.

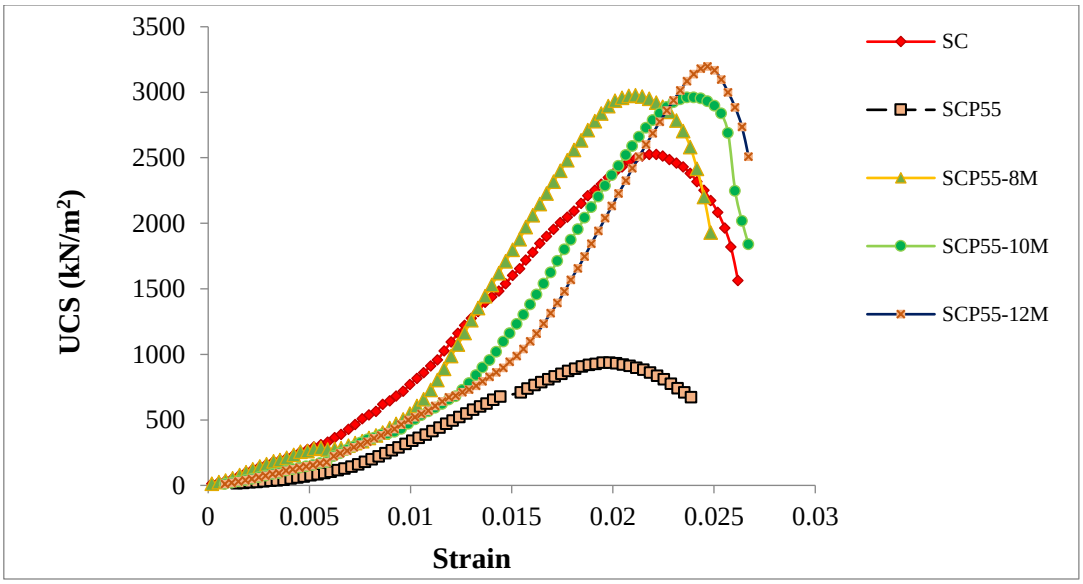

Figure 4.9 Stress-strain characteristics of rammed earth samples treated with alkali-silicate activator after 28 days.

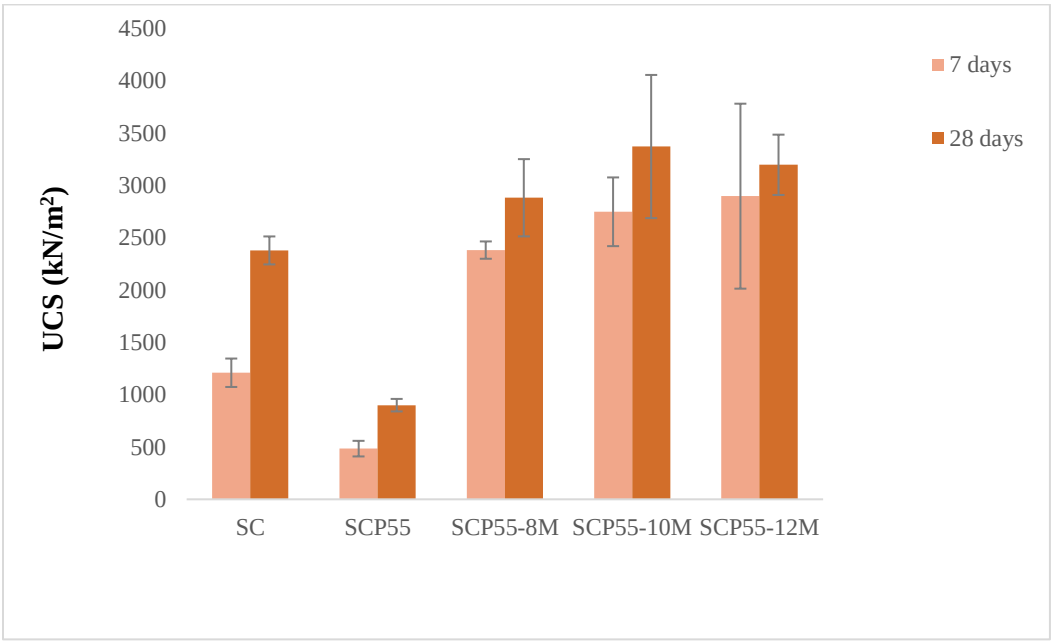

Figure 4.10 Variations in UCS values for RE samples treated with alkali-silicate activator between 7 days and 28 days.

4.6.2 Samples treated with PFA and calcium bentonite

Figures 4.11 and 4.12 illustrate the stress-strain curves of samples treated with various combinations of PC, PFA, and Ca-bentonite, and cured for 7 days and 28 days, respectively. The samples with higher PFA content (i.e., 10% and 20% PFA) exhibited higher UCS values and more brittle behavior compared to the SCP55 sample (with 5% PFA). Hence, the addition of PFA improved stiffness properties of RE samples. Figure 4.13 depicts the difference in the UCS values of 7 days and 28 days cured RE samples corresponding to different design mixes (error bars represent the standard deviation of the measured values). The 7-day cured SCP520 had a comparable UCS value with the control sample SC (1.03 MPa for SCP520 compared to 1.23 MPa for SC), even though the UCS of the SC sample after 28 days was higher than the 28-day cured SCP520 (2.38 MPa to 1.98 MPa). Stabilizing RE samples with 15% percent of Ca-bentonite was effective on their compressive strength. The compressive strength improvement of SCPB5515, SCPB51015, and SCPB52015 was obvious compared to samples SCP55, SCP510, and SCP 520 after 7 days and 28 days of curing indicating the effectiveness of stabilizing with Ca-bentonite. Furthermore, all the samples treated with Ca-bentonite and PFA exhibited a similar compressive strength compared to RE samples treated with alkali-silicate activator. The highest UCS value for this batch was recorded as 3.56 MPa for SCPB51015 after 28 days of curing.

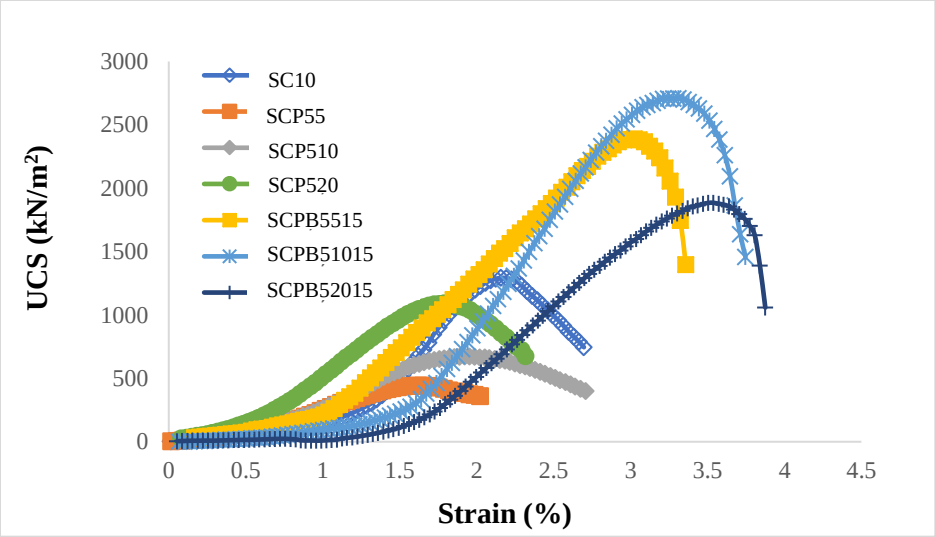

Figure 4.11 Stress-strain characteristics of RE samples treated with PFA and bentonite after 7 days.

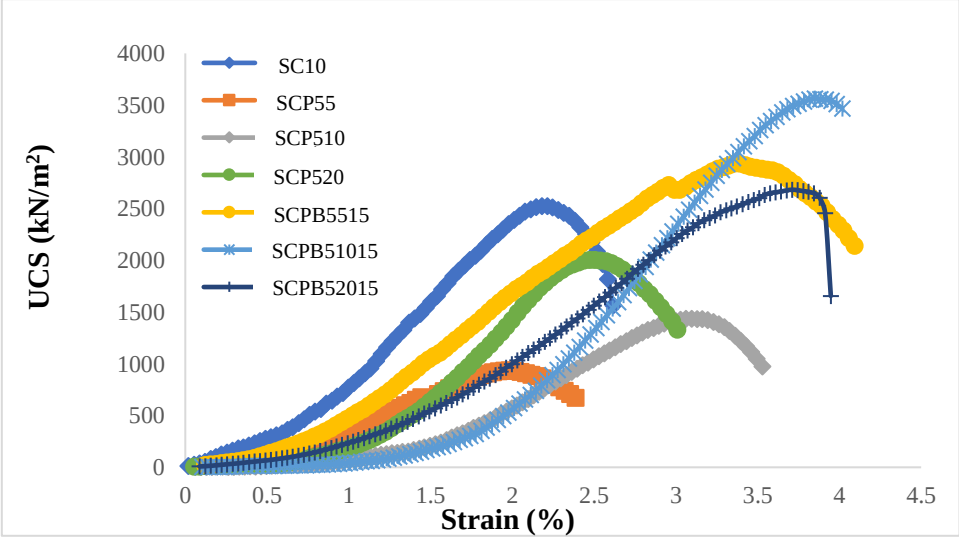

Figure 4.12 Stress-strain characteristics of RE samples treated with PFA and bentonite after 28 days.

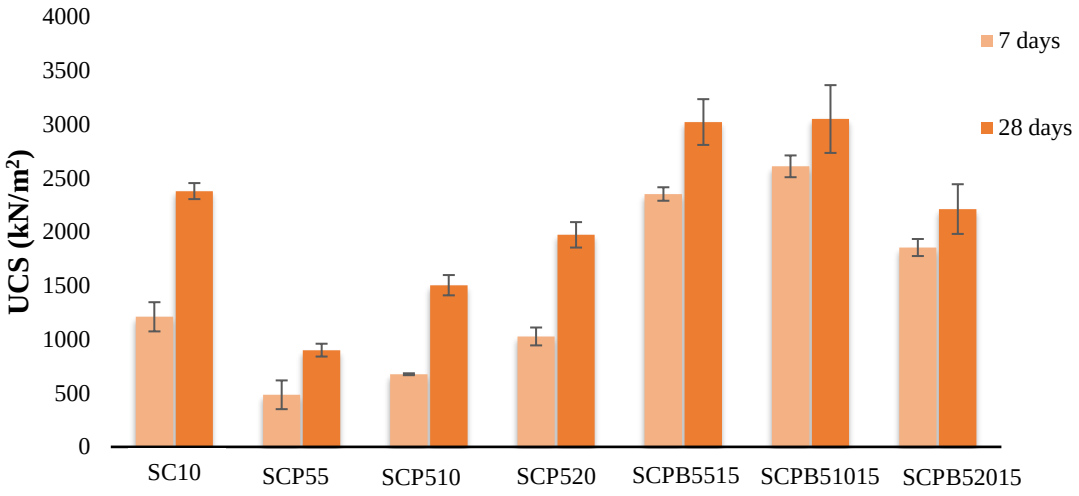

Figure 4.13 Variations in UCS values for RE samples treated with PFA and bentonite between 7 days and 28 days.

4.6.3 Elastic modulus

The elastic modulus of the RE samples and the strain at the ultimate stress were calculated based on the stress-strain characteristics, and the obtained results are provided in Table 4.4. The secant modulus of all samples was calculated at 33.3 % of the highest strength (Upadhyaya, 2016). Similar to the trend in UCS variation**,** the elastic modulus of RE with 5% PC substitution with virgin PFA (i.e., SCP55) also decreased drastically after curing. The specimens with alkali-silicate activator treatment showed an increase in secant modulus values by 2 to 3 times. All samples that were treated with alkali-silicate activator exhibited significantly high elastic modulus. The samples with 10% PFA and 20% PFA without Ca-bentonite exhibited an increase in their secant modulus. Samples stabilized with Ca-bentonite had a higher elasticity modulus compared to the samples without bentonite except for the SCPB52015 at 7 days of curing. However, after 28 days of curing, the secant modulus of the sample was higher than the one without bentonite. Moreover, there was

a steady increase in the mechanical behavior of RE material with the extent of curing indicating the influence of time-dependent chemical reactions and formation of cementation products.

Table 4.4 Elasticity modulus and strain at ultimate stress after 7 days and 28 days.

Sample No.	7 days		28 days	
	Elasticity modulus @ 33.3% of ultimate stress	Strain at ultimate stress	Elasticity modulus @ 33.3% of ultimate stress	Strain at ultimate stress
	MPa	%	MPa	%
SC	2964.99	2.15	3716.4	3.37
SCP55	1958.29	1.62	3196.34	1.98
SCP55-8M	4326.17	2.71	4382.1	3.17
SCP55-10M	4811.86	2.86	5654.16	3.20
SCP55-12M	4659.78	3.19	5411.94	2.64
SCP510	2136.81	1.96	2502.3	3.1
SCP520	4221.81	1.82	4330.54	2.47
SCPB5515	5095.53	3.02	6811.85	3.39
SCPB51015	4454.89	3.31	5313.5	3.32
SCPB52015	2965.83	3.54	4666.32	3.71

4.7 Microstructural examination based on SEM-EDS analysis

4.7.1 Samples treated with the alkali-silicate activator

SEM images and EDS results of different RE samples (viz., SC, SCP55, and SCP55-12M) after 7 days of curing are indicated in Figure 4.14. Figure 4.14a demonstrates that the addition of 10% PC caused the formation of new crystalline products with needle-like morphology. These crystalline products are created through the hydration of anhydrous cement compounds (Alite and Belite) as well as pozzolanic reactions between cement and soil minerals (such as quartz and feldspar). Based on EDS analysis (Figure 4.14b), these compounds have a chemical composition similar to that of calcium silicate hydrate (CSH) crystals present in the concrete systems. Furthermore, there are unreacted soil particles, which is related to partial mobilization of cementation reactions in the system with low PC contents. In the SCP55 sample (Figure 4.14c) the needle-shaped calcium aluminate silicate hydrate (CASH) crystals are observed. However, these

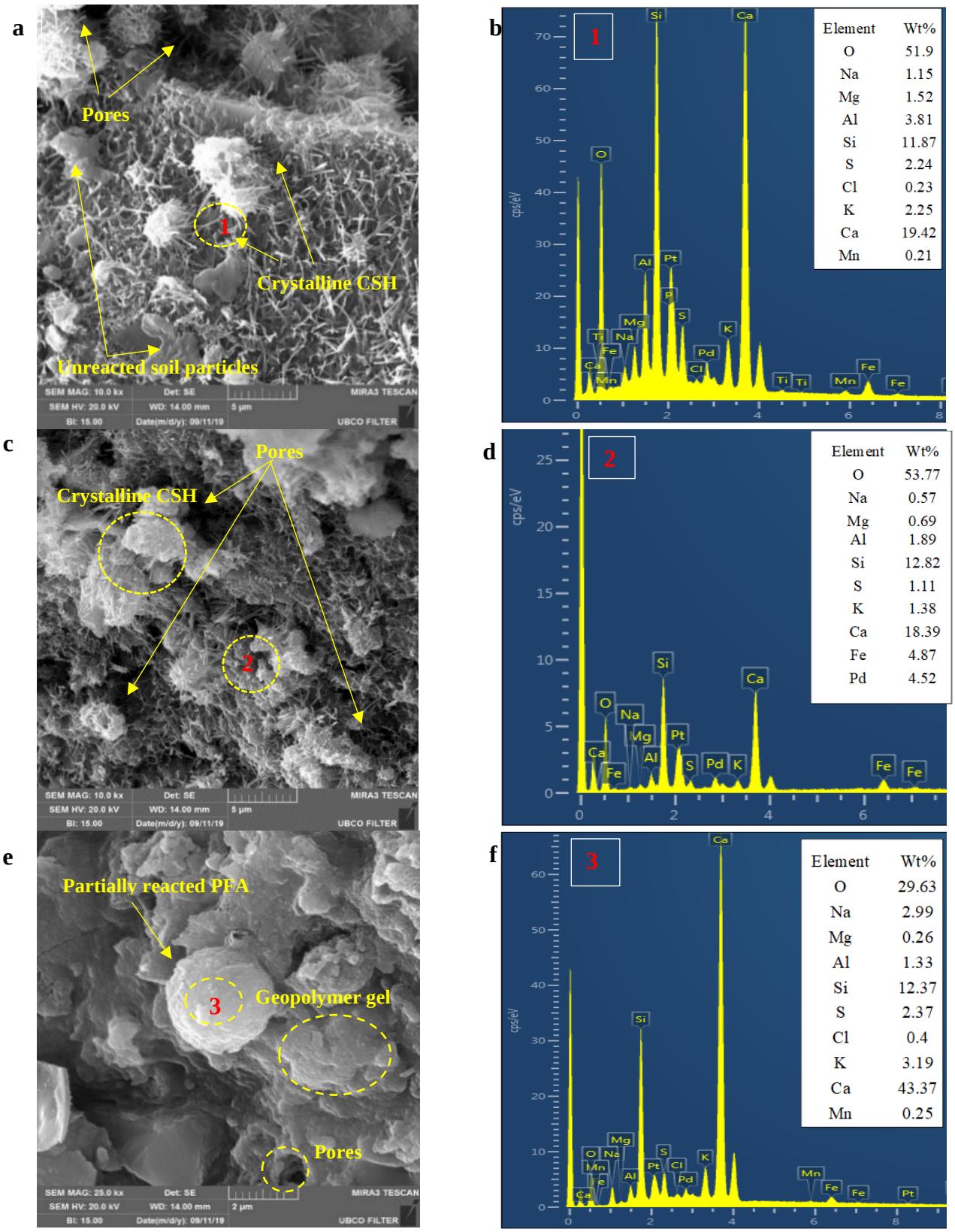

Figure 4.14 SEM images and EDS results of the stabilized RE samples cured for 7 days (a,b) SC, (c,d) SCP55, (e,f) SCP55-12M.

products have more pore spaces and are less dense compared to the 10% PC treated counterpart (SC). The EDS result of these needle-shaped structures (Figure 4.14d) indicated the formation of Ca-Si bonds in the sample. On the other hand, the SEM image of the sample "SCP55-12M" in Figure 4.14e, exhibited a uniform and dense coating of alumino-silicate geopolymer gel. The formation of this gel is due to the alkali-silicate activation of PFA particles in the presence of NaOH and Na_2SiO_3. Even though we can still observe the pores and unreacted PFA, the geopolymerization resulted in a significant strength improvement in the sample, exhibiting a UCS value of 2.9 MPa (Figure 4.8). The EDS spectra of this sample (Figure 4.14f), indicated that the Ca-Si-Al bonds were formed.

Figure 4.15 illustrates the SEM images and EDS spectra of RE samples after 28 days of curing. The morphology of these samples is similar to the samples prepared after 7 days of curing. For the SC and SCP55 samples (shown in Figure 4.15a, c), the additional growth of CSH and CASH compounds is observed in the inter-particle spaces. Therefore, these cementitious compounds undergo further crystallization in a longer curing time which results in the improvement of the mechanical properties of stabilized RE material. However, there are still some unreacted particles and pore spaces in these samples. The EDS results of these samples are depicted in figure 4.15b, d which indicates the presence of Ca-Si-Al bonds after 28 days of curing. In Figure 4.15e, the sample treated with 12 M alkali-silicate activator (SCP55-12M), indicated some pseudo-crystalline compounds on the alumino-silicate geopolymer coating covering the majority of the soil surface. The EDS results of these compounds demonstrated a high concentration of Si and Ca.

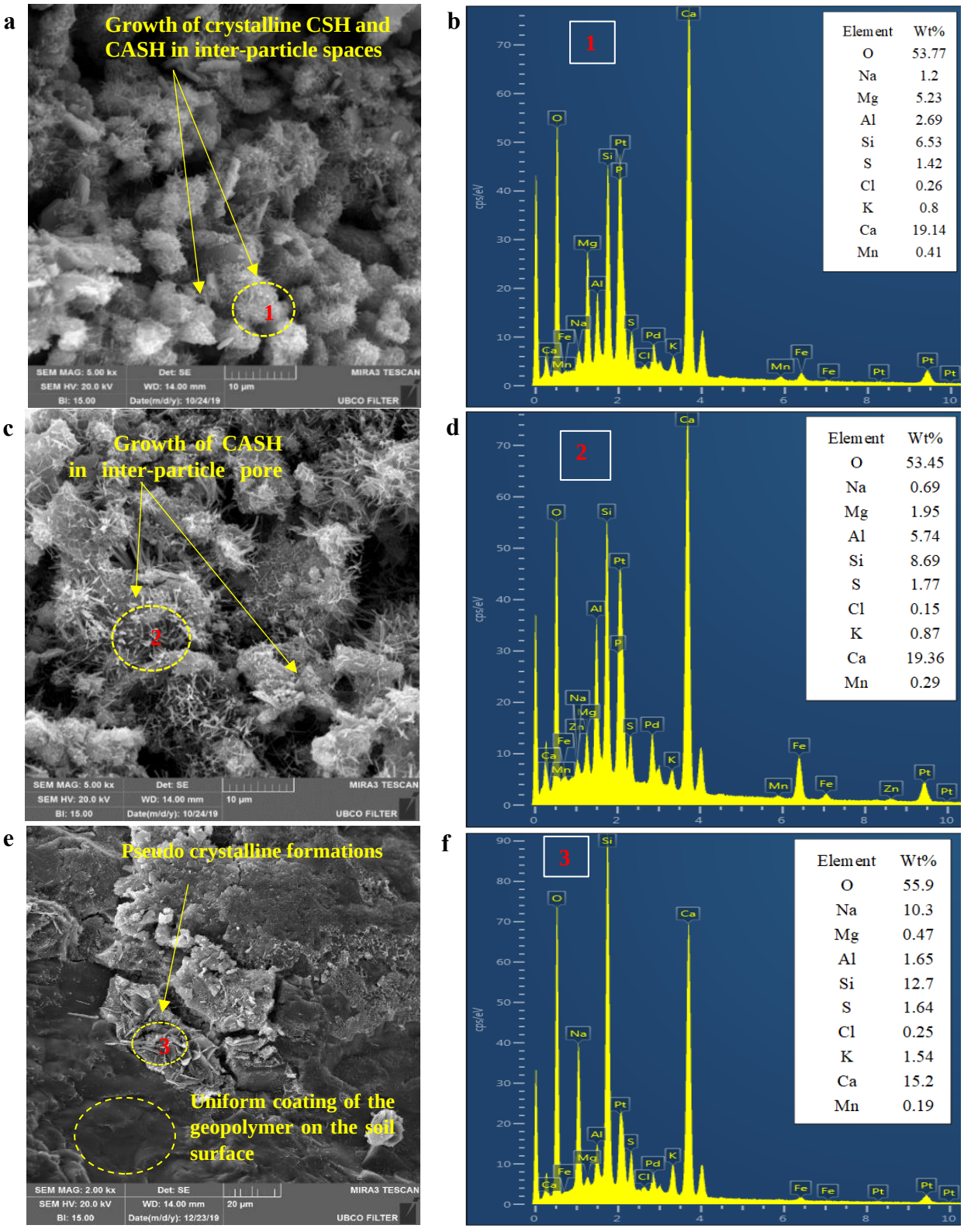

Figure 4.15 SEM images and EDS results of the stabilized rammed earth samples cured for 28 days (a,b) SC, (c,d) SCP55, (e,f) SCP55-12M.

4.7.2 Samples treated with calcium bentonite

The SEM-EDS analysis of RE samples in the second batch is provided in Figure 4.16 which depicts the SCPB52015 sample after 7 days of curing. In this stage of curing some newly formed needle shaped crystals are visible all over the sample that based on the EDS, contain Ca > Si > Al (Figure 4.16 b). After 7 days of curing, there are still some unreacted particles and void spaces with different dimensions (10 to 20 μm) that mostly contain carbon and calcium. Furthermore, the SEM-EDS data of the same sample after 28 days (Figure 4.16 c,d) exhibits less porous surface. The crystalline formations that are observed all over the sample are cementitious products including CSH and CASH (Jha and Sivapullaiah 2015). These cementitious materials could be formed by pozzolanic reactions due to the additional supplement of ions.

The EDS results on these formations revealed that the weight percentage of Si and Al increased during 28 days of curing. The Ca/Si ratio was decreased in CSH formations that can be attributed to the higher compressive strength (Kunther et al. 2017). The SEM image on the sample SCPB51015 after 28 days (Figure 4.16 e) indicated the formation of CSH and CASH crystals with diameters of about 5 μm. The EDS over these structures (Figure 4.16 f) exhibited most of these formations contain Si, Ca, and Al. The weight percentage of Si and Al was higher due to the dissolution of Si and Al that are present in the soil and clay particles and their reaction with OH ions. was also investigated. In the SEM image for the SCP520 sample after 28 days (Figure 4.16 g,h) newly formed structures were detected with more void between the particles. The EDS revealed that these structures have SI, Al, and Ca in their formation however comparing with samples treated with Ca-bentonite, these crystals had less amount of Ca and higher Si in their formation.

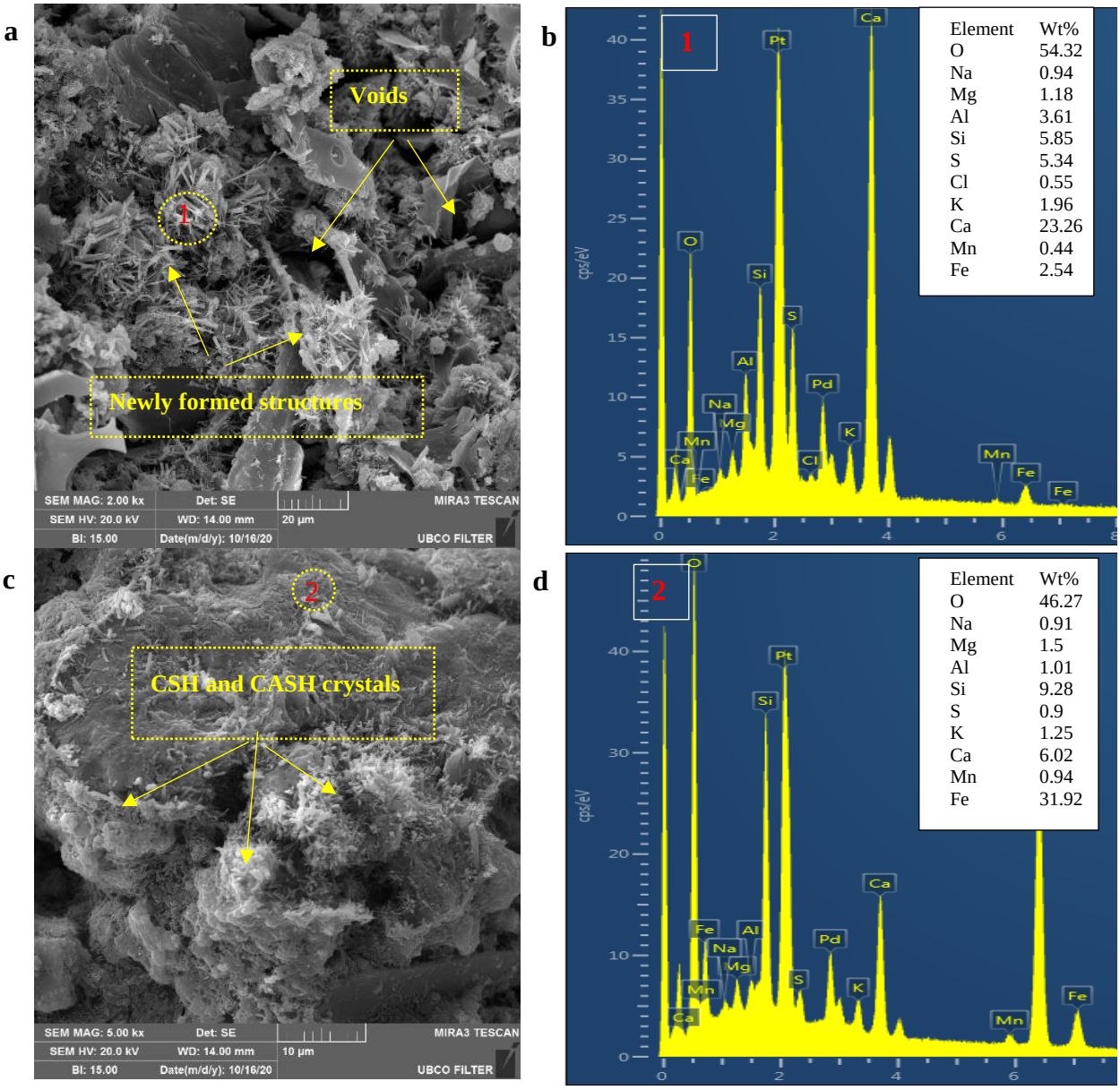

Figure 4.16 SEM images and EDS results of the rammed earth samples (a,b) SCPB 52015 7days, (c,d) SCPB52015 28 days, (e,f) SCPB51015 28 days, (g,h) SCP520.

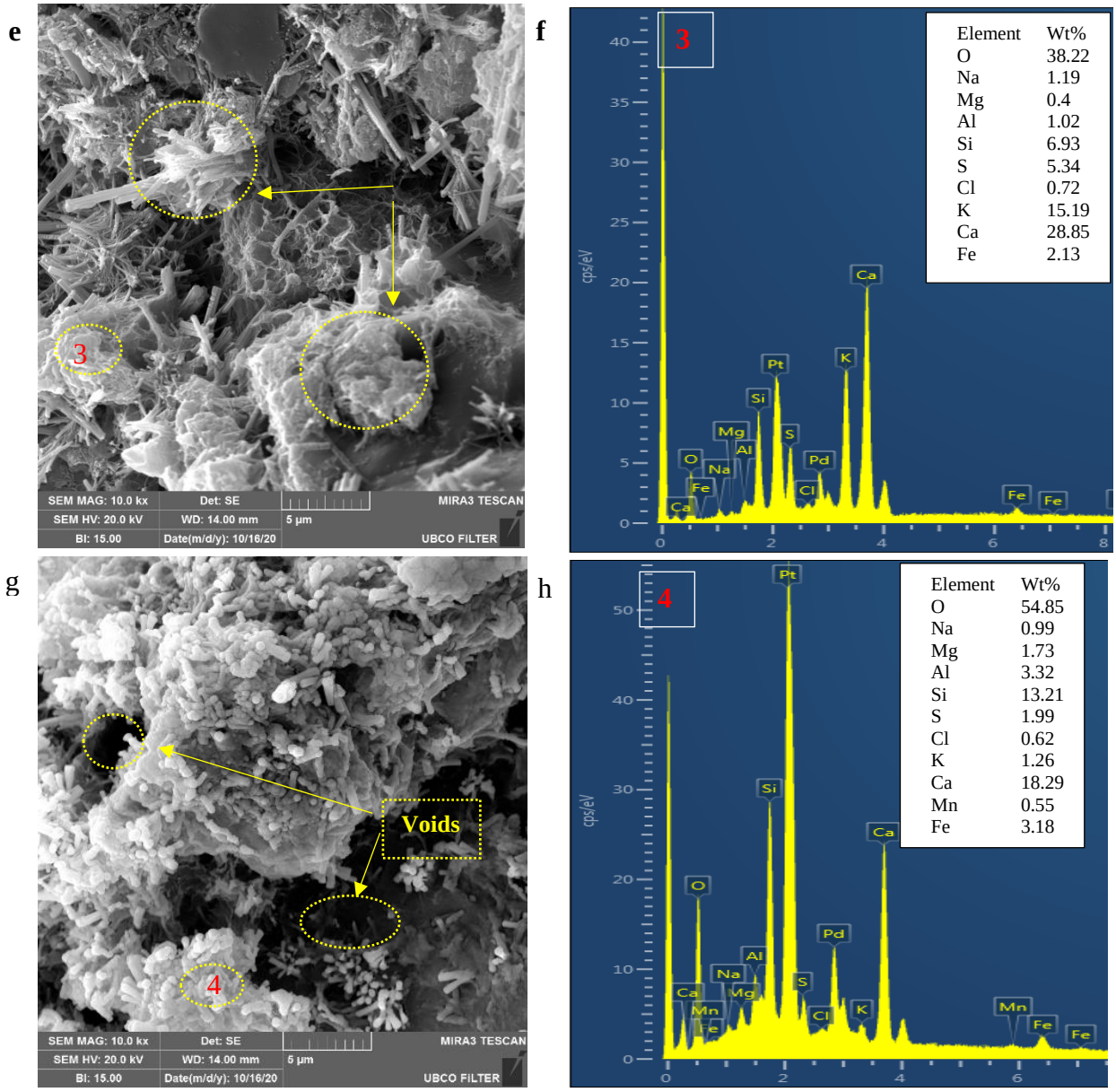

Figure 4.17 continued.

4.8 Freeze-thaw durability properties

The freeze-thaw condition was applied on samples after 28 days of curing. Table 4.5 presents the results of freeze-thaw durability tests, conducted for rammed earth specimens treated with cement, fly ash, and activator solutions before, after 6 cycles, and after 12 cycles of freeze-thaw. In this study, the specimens that were stabilized with PC and PFA exhibited satisfying resilience properties which are attributed to the high stability of the reaction products formed after treatment.

On contrary, the compressive strength of all specimens treated with PFA and activator solutions completely degraded due to weathering effects. The drastic deformation of geopolymer morphology and formation of cracks on its surface is also evident in the SEM images presented in Figure 4.17a,c. Consequently, it can be inferred that reaction products formed by alkali-silicate activation treatment are highly unstable under extreme weathering conditions. Therefore, this recipe can be recommended only for constructing non-load bearing interior building components that are not exposed to extreme climate changes

Besides, the specimens treated with PFA and Ca-bentonite exhibited excellent resilience under freeze-thaw cycles. This can be related to the effectiveness of Ca-bentonite for stabilizing agent. Among these specimens, SCPB51015 showed the highest durability with keeping about 92% of its strength after 12 cycles. The SEM-EDS analysis help to investigate the microstructural properties of the SCPB51015 sample after 12 cycles (Figure 4.17 e,f). There were no cracks identified on the SEM images. The CSH and CASH crystals formed over the sample containing Ca, Si, and Al with the following order of Ca>Si>Al.

Table 4.5 UCS values of samples at different stages after the freeze-thaw durability test.

Sample	Unconfined compressive strength (MPa)		
	Before freeze-thaw	After 6 freeze-thaw cycles	After 12 freeze-thaw cycles
SC	2.4	2.2	3.07
SCP55	0.9	0.94	0.94
SCP55-8M	2.9	Broken	Broken
SCP55-10M	3.37	Broken	Broken
SCP55-12M	2.85	Broken	Broken
SCP510	1.5	-	1.61
SCP520	1.97	-	1.54
SCPB5515	3.02	1.8	2.59
SCPB51015	3.05	2.35	2.79
SCPB52015	2.21	1.78	1.64

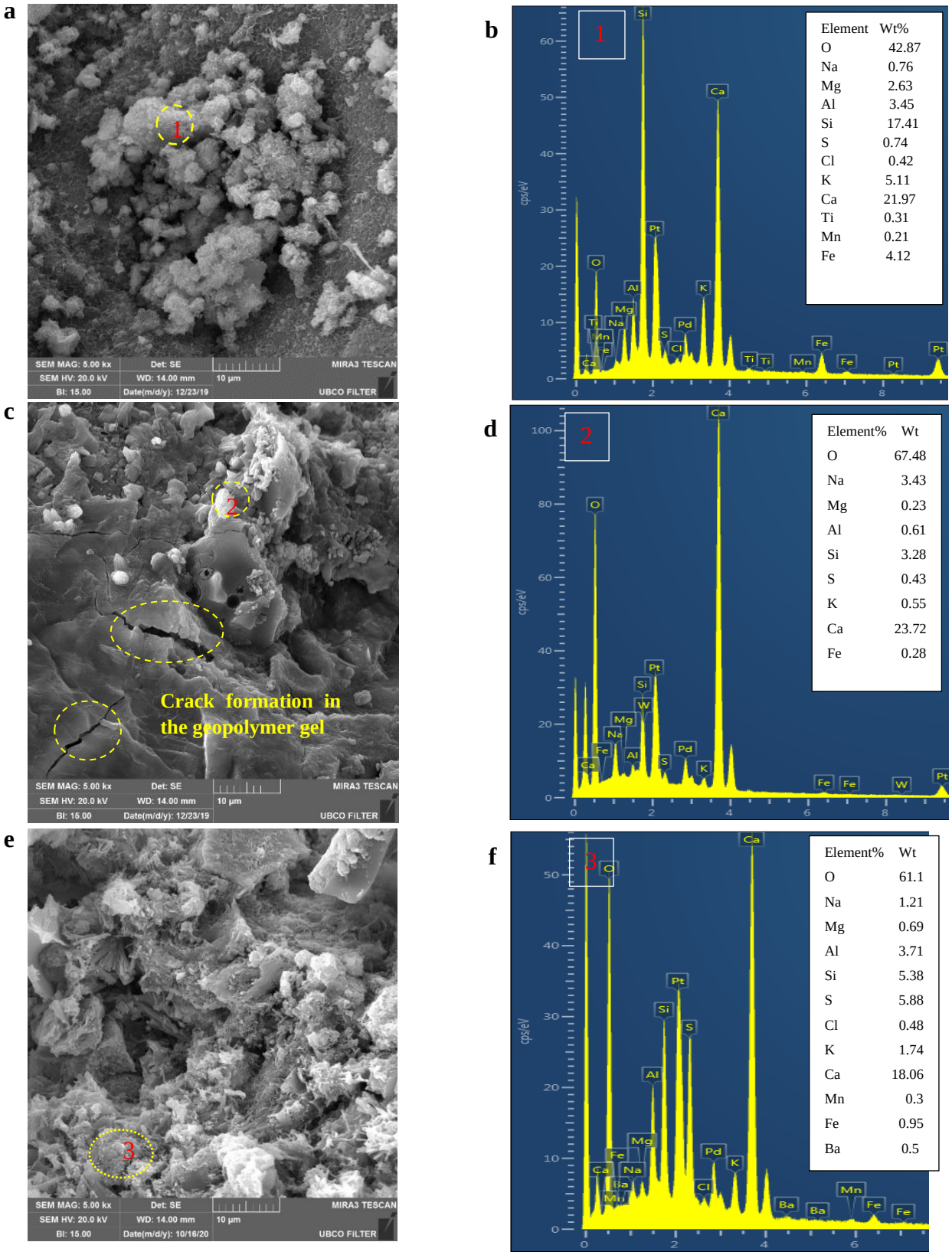

Figure 4.18 SEM images of samples after applying freeze-thaw condition. (a,b) SCP55 (c,d) SCP55-10M (e,f) SCPB51015.

4.9 Molecular characterization of stabilized rammed earth using FTIR

Figure 4.18 shows the FTIR spectra of different stabilized RE samples using PC, PFA, and activator solutions (at different concentrations) corresponding to 28-day curing. The assignments for the characteristic major and minor absorption bands in the spectra are listed in Table 4.6. The single absorption band with maximum peak intensity located at 956 and 1112 cm^{-1} corresponded to the region assigned for asymmetric stretching vibrations of structural Si–O–Si and Si–O–Al bonds (Murmu et al., 2020). The band at about 874 cm^{-1} is attributed to Si–O stretching and –OH bending of Si-OH bonds, and at 598cm^{-1} is related to structural Si–O/Al–O bonds. These characteristic peaks are attributed to the synergetic effect of the behavior of amorphous aluminosilicate compounds present in soil aggregates and binder materials during IR interaction. The broadband at 3424cm^{-1} is due to stretching vibrations of –OH, stretching vibrations of adsorbed water molecules, as well as structural –Si–OH bonds in the aluminosilicate compounds (Andoni et al., 2018). Another two sharp peaks at 1739 cm^{-1} and 1443 cm^{-1} present in all stabilized RE samples is attributed to vibrational mode (O–C–O stretching) of carboxyl (CO_3^{2-}) group in the carbonate species present originally in the fly ash and also formed during treatment and curing processes.

Closer examination of the FTIR spectra revealed that peak intensity of the band assigned to –OH groups (at 3424 cm^{-1}), and carbonate groups (1443 cm^{-1}) increased proportionally with the increasing NaOH concentration from 8M to 12M. This trend was furthermore evident in the peak intensities appearing in the range of 800-1200 cm^{-1} attributed to Si-O-Si and Si-O-Al asymmetric stretching. On contrary to reports of previous studies (Fernández-Jiménez and Palomo, 2005; Dungca and Codilla, 2018), these peaks did not show any behavior of significant shift to the lower or higher wavelength from virgin fly ash to PFA-geopolymer treated rammed earth. Further, two

sharp peaks at around 3000 cm^{-1} (2931 and 2892 cm^{-1}) exhibited by the PFA-geopolymer stabilized RE sample corresponding to 12M NaOH (SCP55-12M) indicated a weakening stretch of the alkene C–H bonds. It confirmed the weaker bonding capacity of the untreated fly ash compared with the optimized PFA-geopolymer (Bruno et al., 2018). Another small band at 1645 cm^{-1} was observed for all samples, indicating the characteristic peak attributed to H–O–H bending mode (H–O–H) of adsorbed water molecules on the surface. It is important to note that a marked decrease of the transmittance occurred for the peaks corresponding to C–H and H–O–H bonds in PFA-geopolymer corresponding to 12M NaOH. Besides, new sharp peaks formed at 1739 cm^{-1} and 1220 cm^{-1} indicated the formation of sodium carbonate by atmospheric carbonation of free NaOH present in excess amounts in the highly concentrated activator solution (Al Bakri Abdullah et al., 2012). Nonetheless, these peaks disappeared after 28 days of curing probably due to the completion of the geopolymerization reaction and full mobilization of the cementation reactions. Thus, the molecular study using FTIR analysis gave supporting evidence for the time-dependent formation of new phases such as the amorphous aluminosilicate gel in the stabilized rammed earth, which in turn caused a dramatic improvement in UCS after 7 days and 28 days-curing periods when compared to the counterparts (control specimens SP and SCP55).

In Figure 4.19, it can be observed that a marked increase of the transmittance occurred for the peaks corresponding to structural hydroxyl groups (between 3000-3600 cm^{-1}) and aluminosilicate groups (between 800-1200 cm^{-1}) for stabilized rammed earth specimens after 12 freeze-thaw durability tests. At the same time, there was an increasing trend of the peak intensity attributed to the carboxyl group in the carbonate species present in all specimens after freeze-thaw cycles. This indicated that the newly formed amorphous aluminosilicate polymer gel was structurally unstable and could not resist the frost action. Moreover, during the freeze-thaw cycles, the atmospheric

interactions caused increased carbonation reactions which also partially contributed to the strength degradation.

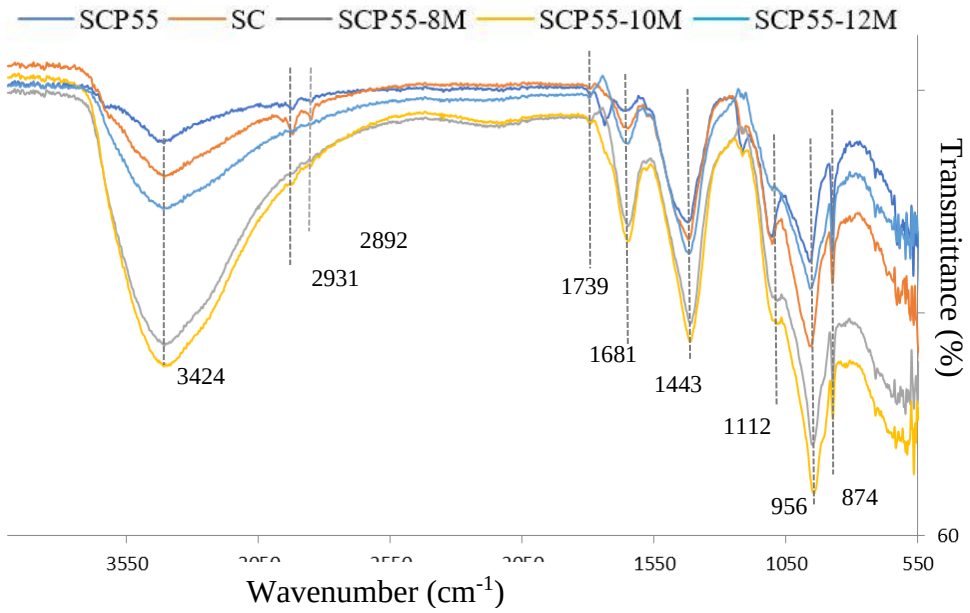

Figure 4.19 Series of FTIR spectra corresponding to rammed earth stabilized using Portland cement, PFA, and activator solutions (at different concentrations) after 28 days curing.

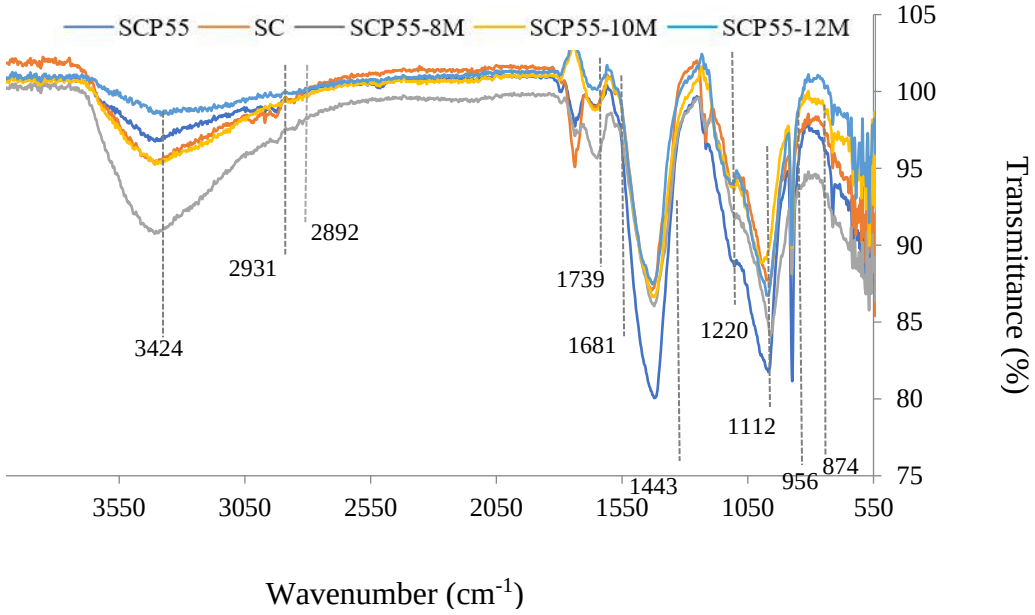

Figure 4.20 Series of FTIR spectra corresponding to rammed earth stabilized using Portland cement, PFA, and activator solutions (at different concentrations) after freeze-thaw durability tests.

Table 4.6 Tentative assignments of characteristic peaks in the IR spectra of stabilized rammed earth.

Wavenumber (cm^{-1})	Band assignment
3646	Hydroxyl (O–H) stretching band of calcium hydroxide species (C–H)
3424	O–H stretching of adsorbed water and –OH groups of –Si–OH groups
2942, 2896	Stretching vibration of alkene C–H bonds in CH_2 groups
1739, 1443, 1220	C=O stretching vibration of CO_3^{2-} group from carboxyl (–COO) group
1645	H–O–H bending vibration of adsorbed water molecules
1112, 956	Asymmetric stretching vibration of the Si–O–Si and Si–O–Al bonds

4.10 Leachate characteristics of stabilized rammed earth

Table 4.7 presents the water-extractable metal concentrations that were measured for PFA, Ca-bentonite, and PFA-treated soils after 28-days curing. To evaluate the potential environmental risks associated with the implementation and service life of PFA-treated samples (upon their interaction with groundwater or infiltrated water), the results were compared with environmental standards. The standard limits were demonstrated in table 4.7 for different hazardous elements from the BC provincial EPA water quality standards for agricultural purposes. It was noticed that the concentration of all hazardous elements except for Cr is below the permissible limit for all the PFA-treated samples. Furthermore, the Mn concentration was below the provided limit only for samples cured with Ca-bentonite. Moreover, due to the extremely low amount of hazardous element content in the raw ash, the leachable concentrations of these elements were only available in trace levels (in µg/kg or ppb, parts per billion). The comparison of the element concentrations in the samples SCP55 and SCP55-10M with the control sample revealed that the concentration of most of the hazardous elements such as Cd, Cr, Cs, Hg, Li, Mo, P, Pb, Sb, Se, V, Zn in SCP55 and Ba, Cd, Cr, Cs, Cu, Hg, Li, Mo, P, Pb, Sb, Se, V, Zn in SCP55-10M were increased after PFA treatment. However, the minimum concentrations of Ba, Co, Cu, Li, Mn, Ni, P, Pb, Sr were belonged to the SCPB5515 sample. Considering the durability and mechanical performance of this sample it can be inferred that treatment of soil samples with PFA and Ca-bentonite was resulted

in enclosing the hazardous impurities within the newly formed cementitious compounds of solidified soil (Zhou et al., 2000).

Table 4.7. Water-leached metal concentrations in PFA, Ca-bentonite, PC, and optimum PFA-treated samples.

Water-leached metal concentrations in parts per billion (µg/kg)								Water quality standard for agriculture (µg/kg)
SAMPLE	**PFA**	**Ca-Bentonite**	**OPC**	**SC**	**SCP55**	**SCP55-10M**	**SCPB5515**	
Ba	148.24	2600.976	1497.285	876.97	169.75	202.56	103.55	n/p
Cd	0.65	0.00	0.10	0.18	1.09	0.67	0.24	5.10
Co	0.70	83.84	2.15	0.87	0.70	0.56	0.16	50.00
Cr	252.81	268.46	161.19	52.70	193.87	213.37	153.82	12.9
Cs	136.90	27.77	33.36	0.16	0.26	0.33	0.61	n/p
Cu	1183.292	4787.04	448.38	683.12	510.29	714.45	19.43	n/p
Hg	53.33	31.14	5.97	2.41	2.79	2.97	6.83	n/p
Li	247.13	54.51	217.08	8.20	14.73	14.29	2.73	2500
Mn	636.32	6938.65	464.07	403.98	382.61	375.21	38.79	200
Mo	625.85	16.47	73.88	10.70	41.42	55.49	47.71	n/p
Ni	4.05	463.06	6.74	3.64	3.16	2.70	1.81	200
P	375.74	3021.08	160.57	251.21	381.43	319.06	215.90	n/p
Pb	14.21	202.06	5.66	6.37	6.69	6.39	0.49	200.00
Sb	1.19	10.26	0.28	0.21	0.59	0.41	1.18	n/p
Se	71.89	0.00	3.07	0.34	3.94	4.26	3.25	n/p
Sr	1476.74	1494.52	15966.08	2386.557	650.84	949.33	636.56	n/p
V	32.21	533.40	2.91	3.37	4.46	3.48	29.14	n/p
Zn	162.20	1874.83	103.64	157.68	192.82	180.31	315.23	n/p

Note: n/p- not provided

Chapter 5: Conclusions

5.1 Summary

The overall goal of this research was to develop innovative waste-to-product technologies for valorization of pulp mill solid residues as eco-friendly alternatives to cement, and thereby to enable the conservation of natural resources, reduce the environmental footprints, and also save valuable landfill spaces for other non-beneficial waste materials. The various mix designs of RE material were developed by incorporating local soil, PC, Ca-bentonite, and PFA with different combinations of alkali-silicate activator solution (for geopolymerization of ash). The compressive strength and durability properties of different RE design mixtures were determined in terms of UCS variations after moist curing, and standard freeze-thaw cycles, respectively. Further, detailed microstructural analysis with the aid of SEM-EDS and FTIR analysis was also performed to have a better insight into the underlying reaction cementation mechanisms in RE design mixtures which caused strength and durability changes during the curing process and freeze-thaw cycles. The developed novel mix design technology for sustainable rammed earth, using pulp mill fly ash and alkali-silicate activator as a partial replacement for Portland cement, provides a promising sustainable material for load-bearing as well as non-load-bearing internal structures, partitions, and panel walls, etc. which are not directly exposed to seasonal climatic variations and harsh weather conditions. The mix design using Ca-bentonite and PFA can also be a suitable material as a PC replacement in the structures in cold climate conditions as it was durable under continuous freezing and thawing cycles.

5.2 Major findings

The purpose of the present study was to develop a novel mix design technology for sustainable RE material by incorporating PFA as a partial replacement for PC. Based on the obtained experimental results, the following are major conclusions of this study.

5.2.1 Alkali-silicate activation of PFA

The RE specimens treated with 5% PC and 5% PFA (i.e., 50% cement replacement by fly ash) and different concentrations of alkali-silicate activators were evaluated for the variations in strength and durability properties compared to the control specimens using 10% cement as stabilizer.

- Physico-chemical and toxicological properties of PFA are favorable for sustainable application as a cementitious binder in construction.
- Alkali-silicate activation of PFA significantly affects the strength development as a function of time and activator chemistry.
- With the extent of curing, the RE samples treated with activated PFA becomes stiffer due to time-dependent geopolymerization reaction and cementation phenomena.
- The microstructural evaluation revealed the formation of a uniform and dense coating of alumino-silicate geopolymer gel and some calcium-alumino-silicate crystals on the soil matrix.
- The durability of RE samples treated with as-received PFA was satisfactory after 12 freeze-thaw cycles, whereas those incorporated with PFA-geopolymer exhibited poor frost resilience properties.
- The ICP analysis exhibited that the trace element concentration in the SCP55 and SCP55-10M samples were below the standard level, except for the Cr and Mn. The

element concentrations were only available in trace levels (in µg/kg or ppb, parts per billion) due to the extremely low amount of hazardous element content in the raw ash.

5.2.2 Calcium bentonite and PFA treatment without alkali-silicate activation

The RE samples stabilized with different PFA dosage such as 5%, 10%, and 20%, along with and without additional 15% bentonite were investigated by UCS test, freeze-thaw durability test, and microstructural analysis.

- Increasing the PFA weight percentage from 5% to 20% in samples without bentonite improved the compression strength of RE samples after their curing time which indicates the suitability of PFA as a cementitious material for RE stabilization. However, the compressive strength of 28 days cured SCP520 sample was less than that of control sample (28 days SC sample).
- The samples treated with PFA and Ca-bentonite exhibited a considerable improvement in their mechanical performance after 7 days and 28 days of curing, compared to samples without Ca-bentonite. This highlights the suitability of Ca-bentonite along with PFA for RE stabilization.
- The samples with 5% PFA and 10% PFA with Ca-bentonite were chosen as the optimum mix designs as their strength improvements were significant after 28 days of curing.
- All the samples treated without alkali-silicate activator were durable under freeze-thaw conditions. The SCPB51015 had the best performance with minimum strength loss.
- The microstructural investigations of treated samples with SEM- EDS revealed that the pozzolanic reactions formed CSH and CASH crystals in the samples. The samples treated with Ca-bentonite were coated uniformly with fewer voids in between

particles. The crystals were mostly contained Ca, Si, and Al in the following order of Ca> Si>Al.

- Based on the ICP analysis for 5% PFA and 15% Ca-bentonite optimized recipe compared with the control sample (10% PC), the minimum concentrations of Ba, Co, Cu, Li, Mn, Ni, P, Pb, Sr were noticed. Additionally, the concentration of trace elements except for Cr was below the standard limit for this sample that was due to the immobilization of metals in the new compounds formed by cementation reactions. Hence, this sample is environmentally safe.

5.3 Limitations and future works

The durability of RE structures is investigated in the past years considering different variations and having PC in the mixture was known to be an effective method. Partially substitution of PC with secondary by-products can be a problematic issue that needs multiple considerations and facing some limitations. A description of some of these limitations and recommendations for future studies are as follows:

In this research, the alkali-silicate activation of PFA and using Ca-bentonite as a stabilizer was employed. More research is required in the sustainable rammed earth technology with a focus on further improvement of the freeze-thaw durability of developed RE design mixes by incorporating additional stable binder components.

Curing of samples treated with Alkali-silicate activator was conducted at room temperature. The influence of curing conditions can be assessed by performing multiple temperatures and humidity percentages.

The 28 days of curing was considered as the maximum curing period. Based on the obtained results, the improvement in the mechanical performance of RE mix designs from 7 days to 28 days was noticed. A further investigation is required to assess the RE performance in longer curing periods.

All RE samples were compacted on a laboratory scale in a specific dimension. The various mix designs can be prepared based on greater dimensions to evaluate the effect of size on the RE performance.

The optimum amount of PFA with a constant 15% Ca-bentonite was found in this study. Various combinations of Ca-bentonite and higher PFA percentages can be used in RE mix designs to assess the characteristics of samples.

The alkali-silicate activators were used in a constant ratio of 2:1 Na_2SiO_3 to NaOH and three different molarities for the NaOH solution. More combinations of alkali-silicate activators with different NaOH concentrations can be used to assess the mechanical improvement of RE mix designs.

The standard freeze-thaw cycle was used in this study to evaluate the durability performance of the RE mix designs. Evaluation of the optimum mix design under other durability experiments such as spray test, wire brush test, drip test is recommended for future research studies.

Evaluating the plastic behaviour of the developed recipe and the material used in this study is recommended for the future work.

Bibliography

Ahmadi, B., and W. Al-Khaja. 2001. "Utilization of Paper Waste Sludge in the Building Construction Industry." *Resources, Conservation and Recycling* 32 (2): 105–13. https://doi.org/10.1016/S0921-3449(01)00051-9.

Andoni, Adelaida, Eda Delilaj, Fatos Ylli, Krenaida Taraj, Arjan Korpa, Kledi Xhaxhiu, and Armand Çomo. 2018. "FTIR Spectroscopic Investigation of Alkali-Activated Fly Ash: Atest Study." *Zastita Materijala* 59 (4): 539–42. https://doi.org/10.5937/zasmat1804539a.

Arrigoni, Alessandro, Renato Pelosato, Giovanni Dotelli, Christopher T.S. Beckett, and Daniela Ciancio. 2017. "Weathering's Beneficial Effect on Waste-Stabilised Rammed Earth: A Chemical and Microstructural Investigation." *Construction and Building Materials* 140 (June): 157–66. https://doi.org/10.1016/j.conbuildmat.2017.02.009.

ASTM-D-2216-19. 2019. "Standard Test Method for Laboratory Determination of Water (Moisture) Content of Soil and Rock by Mass." *ASTM International*, no. January: 1–5. https://doi.org/10.1520/D2216-19.

ASTM C128. 2015. "Standard Test Method for Relative Density (Specific Gravity) and Absorption of Fine Aggregate." *ASTM International, West Conshohocken, PA, USA* i: 6. https://doi.org/10.1520/C0128-15.2.

ASTM D2487-17. 2017. "Standard Practice for Classification of Soils for Engineering Purposes (Unified Soil Classification System), ASTM International, West Conshohocken, PA, 2017, Www.Astm.Org." *ASTM International, West Conshohocken, PA, USA* D2487-17: 1–10. https://doi.org/10.1520/D2487-17.

ASTM D2974-20e1. 2020. "Standard Test Methods for Determining the Water (Moisture) Content

, Ash Content, and Organic Material of Peat and Other Organic Soils." *ASTM International*, 1–5. https://doi.org/10.1520/D2974-20E01.2.

ASTM D4972. 2019. "Standard Test Methods for PH of Soils." *Astm*, 1–6. https://doi.org/10.1520/D4972-19.2.

ASTM D5890 − 19. 2019. "Standard Test Method for Swell Index of Clay Mineral Component of Geosynthetic." *Annual Book of ASTM Standards*, 20–23. https://doi.org/10.1520/D5890-19.2.

ASTM D7928-16. 2016. "Standard Test Method for Particle-size Distribution (Gradation) of Fine-grained Soils Using the Sedimentation (Hydrometer) Analysis." *ASTM International*, 1–25. https://doi.org/10.1520/D7928-17.

ASTM D854. 2014. "Standard Test Methods for Specific Gravity of Soil Solids by Water Pycnometer." *Astm* 2458000 (C): 1–7. https://doi.org/10.1520/D0854-10.2.

Aymerich, F., L. Fenu, and P. Meloni. 2012. "Effect of Reinforcing Wool Fibres on Fracture and Energy Absorption Properties of an Earthen Material." *Construction and Building Materials* 27 (1): 66–72. https://doi.org/10.1016/j.conbuildmat.2011.08.008.

Bakri Abdullah, Mohd Mustafa Al, Kamarudin Hussin, Mohamed Bnhussain, Khairul Nizar Ismail, Zarina Yahya, and Rafiza Abdul Razak. 2012. "Fly Ash-Based Geopolymer Lightweight Concrete Using Foaming Agent." *International Journal of Molecular Sciences* 13 (6): 7186–98. https://doi.org/10.3390/ijms13067186.

Beckett, C. T.S., P. A. Jaquin, and J. C. Morel. 2020. "Weathering the Storm: A Framework to Assess the Resistance of Earthen Structures to Water Damage." *Construction and Building*

Materials 242 (May): 118098. https://doi.org/10.1016/j.conbuildmat.2020.118098.

Bergaya, F., K. Beneke, R.W. Berry, G. Lagaly, and K.B. Tankersley. 2013. "Clay Science." https://doi.org/10.1016/b978-0-08-098258-8.00028-6.

Berge, B. 2009. *The Ecology of Building Materials*. 2nd ed. Elsevier Science. https://books.google.ca/books?hl=en&lr=&id=LswsBgAAQBAJ&oi=fnd&pg=PR2&ots=ija315AiyB&sig=MLjHiOFxYYYp9ehBmtO5ClwvF5w&redir_esc=y#v=onepage&q&f=false.

Bhatt, Arpita, Sharon Priyadarshini, Aiswarya Acharath Mohanakrishnan, Arash Abri, Melanie Sattler, and Sorakrich Techapaphawit. 2019. "Physical, Chemical, and Geotechnical Properties of Coal Fly Ash: A Global Review." *Case Studies in Construction Materials* 11: e00263. https://doi.org/10.1016/j.cscm.2019.e00263.

Bruno, Agostino Walter, Céline Perlot, Joao Mendes, and Domenico Gallipoli. 2018. "A Microstructural Insight into the Hygro-Mechanical Behaviour of a Stabilised Hypercompacted Earth." *Materials and Structures/Materiaux et Constructions* 51 (1). https://doi.org/10.1617/s11527-018-1160-9.

Bui, Q.-B., E Prud'homme, .A.-C. Grillet, and N. Prime. 2018. "An Experimental Study on Earthen Materials Stabilized by Geopolymer." In *Cement and Concrete Research*, 1–7. https://doi.org/10.1007/978-981-10-6713-6.

Bui, Q. B., J. C. Morel, B. V. Venkatarama Reddy, and W. Ghayad. 2009. "Durability of Rammed Earth Walls Exposed for 20 Years to Natural Weathering." *Building and Environment* 44 (5): 912–19. https://doi.org/10.1016/j.buildenv.2008.07.001.

Bui, Quoc-bao, and Jean-claude Morel. 2009. “Assessing the Anisotropy of Rammed Earth.” *Construction and Building Materials* 23 (9): 3005–11. https://doi.org/10.1016/j.conbuildmat.2009.04.011.

Bui, Quoc Bao, Jean Claude Morel, Stéphane Hans, and Nicolas Meunier. 2009. “Compression Behaviour of Non-Industrial Materials in Civil Engineering by Three Scale Experiments: The Case of Rammed Earth.” *Materials and Structures/Materiaux et Constructions* 42 (8): 1101–16. https://doi.org/10.1617/s11527-008-9446-y.

Bui, T.-T, Q.B. Bui, A Limama, and S Maximilienc. 2013. “Failure of Rammed Earth Walls: From Observations to Quantifications.” *Construction and Building Materials* volume 51: 295–302. https://doi.org/https://doi.org/10.1016/j.conbuildmat.2013.10.053.

Bui, T. T., Q. B. Bui, A. Limam, and S. Maximilien. 2014. “Failure of Rammed Earth Walls: From Observations to Quantifications.” *Construction and Building Materials* 51: 295–302. https://doi.org/10.1016/j.conbuildmat.2013.10.053.

Burroughs, Steve. 2008. “Soil Property Criteria for Rammed Earth Stabilization.” *Journal of Materials in Civil Engineering* 1561 (2): 1–2. https://doi.org/10.1061/(ASCE)0899-1561(2008)20.

———. 2010. “Recommendations for the Selection, Stabilization, and Compaction of Soil for Rammed Earth Wall Construction.” *Journal of Green Building* 5 (1): 101–14. https://doi.org/10.3992/jgb.5.1.101.

Carvalho, C., de, A. L. Brasil, P. da Silva, and C. M. Gómez. 2015. “Novel Approach to Consolidation Theory of Structured and Collapsible Soils.” *American Society of Civil Engineers.*

Chauhan, Mahipal Singh, Satyendra Mittal, and Bijayananda Mohanty. 2008. “Performance Evaluation of Silty Sand Subgrade Reinforced with Fly Ash and Fibre.” *Geotextiles and Geomembranes* 26 (5): 429–35. https://doi.org/10.1016/j.geotexmem.2008.02.001.

Cherian, Chinchu, and Sumi Siddiqua. 2019. “Pulp and Paper Mill Fly Ash: A Review.” *Sustainability (Switzerland)* 11 (16): 1–16. https://doi.org/10.3390/su11164394.

Chusilp, Nuntachai, Chai Jaturapitakkul, and Kraiwood Kiattikomol. 2009. “Utilization of Bagasse Ash as a Pozzolanic Material in Concrete.” *Construction and Building Materials* 23 (11): 3352–58. https://doi.org/10.1016/j.conbuildmat.2009.06.030.

Ciancio, D. (Ed.), and C. (Ed.). Beckett. 2015. *Rammed Earth Construction.* London: CRC Press. https://doi.org/https://doi-org.ezproxy.library.ubc.ca/10.1201/b18046.

Cristelo, Nuno, Stephanie Glendinning, Lisete Fernandes, and Amândio Teixeira Pinto. 2012. “Effect of Calcium Content on Soil Stabilisation with Alkaline Activation.” *Construction and Building Materials* 29: 167–74. https://doi.org/10.1016/j.conbuildmat.2011.10.049.

Cristelo, Nuno, Stephanie Glendinning, Tiago Miranda, Daniel Oliveira, and Rui Silva. 2012. “Soil Stabilisation Using Alkaline Activation of Fly Ash for Self Compacting Rammed Earth Construction.” *Construction and Building Materials* 36: 727–35. https://doi.org/10.1016/j.conbuildmat.2012.06.037.

D560-12. 2012. “ASTM D560-96 Standard Test Methods for Freezing and Thawing Compacted Soil-Cement Mixtures” i: 1–6. https://doi.org/10.1520/D0560.

Dananaj, Ivan, Jana Frankovská, and Ivan Janotka. 2005. “The Influence of Smectite Content on Microstructure and Geotechnical Properties of Calcium and Sodium Bentonites.” *Applied*

Clay Science 28 (1): 223–32. https://doi.org/https://doi.org/10.1016/j.clay.2004.02.006.

Dong, Xiang, Veronica Soebarto, and Michael Griffith. 2014a. "Achieving Thermal Comfort in Naturally Ventilated Rammed Earth Houses." *Building and Environment* 82: 588–98. https://doi.org/10.1016/j.buildenv.2014.09.029.

———. 2014b. "Strategies for Reducing Heating and Cooling Loads of Uninsulated Rammed Earth Wall Houses." *Energy and Buildings* 77: 323–31. https://doi.org/10.1016/j.enbuild.2014.03.031.

Dungca, Jonathan R., and Edward Ephrem T. Codilla. 2018. "Fly-Ash-Based Geopolymer as Stabilizer for Silty Sand Embankment Materials." *International Journal of GEOMATE* 14 (46): 143–49. https://doi.org/10.21660/2018.46.7181.

Edeh, Joseph Ejelikwu, Isaac Olufemi Agbede, and Audu Tyoyila. 2014. "Evaluation of Sawdust Ash-Stabilized Lateritic Soil as Highway Pavement Material." *Journal of Materials in Civil Engineering* 26 (2): 367–73. https://doi.org/10.1061/(ASCE)MT.1943-5533.0000795.

Faubert, Patrick, Simon Barnabé, Sylvie Bouchard, Richard Côté, and Claude Villeneuve. 2016. "Pulp and Paper Mill Sludge Management Practices: What Are the Challenges to Assess the Impacts on Greenhouse Gas Emissions?" *Resources, Conservation and Recycling* 108: 107–33. https://doi.org/10.1016/j.resconrec.2016.01.007.

Fernández-Jiménez, A., and A. Palomo. 2005. "Mid-Infrared Spectroscopic Studies of Alkali-Activated Fly Ash Structure." *Microporous and Mesoporous Materials* 86 (1–3): 207–14. https://doi.org/10.1016/j.micromeso.2005.05.057.

Frans Lamers, Marcel Cremers, Doris Matschegg, Christoph Schmidl, Kirsten Hannam, Paul

Hazlett, Sebnem Madrali, Birgitte Primdal Dam, Roberta Roberto, Rob Mager, Kent Davidsson, Nicolai Bech, Hans-Joachim Feuerborn, Angelo Saraber. 2018. “Options for Increased Use of Ash from Biomass Combustion and Co-Firing.” *IEA Bioenergy*.

Ganesan, K., K. Rajagopal, and K. Thangavel. 2007. “Evaluation of Bagasse Ash as Supplementary Cementitious Material.” *Cement and Concrete Composites* 29 (6): 515–24. https://doi.org/10.1016/j.cemconcomp.2007.03.001.

Grau, Francisco, Hyunwook Choo, Jong Wan Hu, and Jongwon Jung. 2015. “Engineering Behavior and Characteristics of Wood Ash and Sugarcane Bagasse Ash.” *Materials* 8 (10): 6962–77. https://doi.org/10.3390/ma8105353.

Guettala, A. 2006. “Durability Study of Stabilized Earth Concrete under Both Laboratory and Climatic Conditions Exposure” 20: 119–27. https://doi.org/10.1016/j.conbuildmat.2005.02.001.

Hall, Matthew, and David Allinson. 2009. “Analysis of the Hygrothermal Functional Properties of Stabilised Rammed Earth Materials.” *Building and Environment* 44 (9): 1935–42. https://doi.org/10.1016/j.buildenv.2009.01.007.

Hall, Matthew, and Youcef Djerbib. 2004. “Rammed Earth Sample Production : Context , Recommendations and Consistency” 18: 281–86. https://doi.org/10.1016/j.conbuildmat.2003.11.001.

Hall, Matthew R. 2007. “Assessing the Environmental Performance of Stabilised Rammed Earth Walls Using a Climatic Simulation Chamber.” *Building and Environment* 42 (1): 139–45. https://doi.org/10.1016/j.buildenv.2005.08.017.

Hall, Matthew R, Nottingham Park, Rick Lindsay, and Meror Krayenhoff. 2012. *Modern Earth Buildings: Materials, Engineering, Constructions and Applications*. Elsevier.

Hameed AM., Rawdhan RR., Al-Mishhadani SA. 2017. "Influence of Various Factors on the Production of Geopolymer Mortar." *Arch Sci* 1 (3): 111.

Hardjito, D, Steenie E Wallah, D. M. J. Sumajouw, and B Vijaya Rangan. 2004. "Factors Influencing the Compressive Strength of Fly Ash-Based Geopolymer Concrete." *Civil Engineering ...* 6 (2): 88–93. http://www.freepatentsonline.com/article/Civil-Engineering-Dimension/170455954.html.

Hardjito, Djwantoro, and B Vijaya Rangan. 2005. "Development and Properties of Low-Calcium Fly Ash-Based Geopolymer Concrete." *Research Report GC,* 94. http://www.geopolymer.org/fichiers_pdf/curtin-flyash-GP-concrete-report.pdf.

Heathcote, K. A. 1995. "Durability of Earthwall Buildings." *Construction and Building Materials* 9 (3): 185–89. https://doi.org/10.1016/0950-0618(95)00035-E.

Hu, Mingyu, Xiaomin Zhu, and Fumei Long. 2009. "Alkali-Activated Fly Ash-Based Geopolymers with Zeolite or Bentonite as Additives." *Cement and Concrete Composites* 31 (10): 762–68. https://doi.org/https://doi.org/10.1016/j.cemconcomp.2009.07.006.

Jain, Deepak, Abhijit Mukherjee, Hannah Porter, and Joshua Blake. 2019. "Enhanced Thermal Resistance of Rammed Earth Blocks with Recycled Industry By-Products." *International Journal of Thermal Sciences* 138 (August 2017): 447–58. https://doi.org/10.1016/j.ijthermalsci.2019.01.017.

Jaiswal, Mrityunjay, and Bindhu Lal. 2017. "Stabilization of Clayey Soil with Garlic Skin and

Rice Husk Ash for Flexible Pavement Construction." *Geotechnical Testing Journal* 40 (6): 1071–82. https://doi.org/10.1520/GTJ20160227.

Jaquin, P. A., C. E. Augarde, D. Gallipoli, and D. G. Toll. 2009. "The Strength of Unstabilised Rammed Earth Materials." *Géotechnique* 59 (5): 487–90. https://doi.org/10.1680/geot.2007.00129.

Jayasinghe, C., and N. Kamaladasa. 2007. "Compressive Strength Characteristics of Cement Stabilized Rammed Earth Walls." *Construction and Building Materials* 21 (11): 1971–76. https://doi.org/10.1016/J.CONBUILDMAT.2006.05.049.

Kariyawasam, K. K.G.K.D., and C. Jayasinghe. 2016. "Cement Stabilized Rammed Earth as a Sustainable Construction Material." *Construction and Building Materials* 105: 519–27. https://doi.org/10.1016/j.conbuildmat.2015.12.189.

Lake, Craig B., Mohammed Al Mala Yousif, and Reza J. Jamshidi. 2017. "Examining Freeze/Thaw Effects on Performance and Morphology of a Lightly Cemented Soil." *Cold Regions Science and Technology* 134: 33–44. https://doi.org/10.1016/j.coldregions.2016.11.006.

Leong, Hsiao Yun, Dominic Ek Leong Ong, Jay G. Sanjayan, and Ali Nazari. 2018. "Strength Development of Soil-Fly Ash Geopolymer: Assessment of Soil, Fly Ash, Alkali Activators, and Water." *Journal of Materials in Civil Engineering* 30 (8). https://doi.org/10.1061/(ASCE)MT.1943-5533.0002363.

Li, Zhuguo, Toshihiko Ohnuki, and Ko Ikeda. 2016. "Development of Paper Sludge Ash-Based Geopolymer and Application to Treatment of Hazardous Water Contaminated with Radioisotopes." *Materials* 9 (8). https://doi.org/10.3390/ma9080633.

Liu, Qiang, and Liping Tong. 2017. “Engineering Properties of Unstabilized Rammed Earth with Different Clay Contents.” *Journal Wuhan University of Technology, Materials Science Edition* 32 (4): 914–20. https://doi.org/10.1007/s11595-017-1690-y.

Liu, Xiangwei, Mingyu Hu, Shujun Ke, Chao Fu, Xingguo Guo, and Xiaochun Ye. 2018. “A Novel Rammed Earthen Material Stabilized with Steel Slags.” *Construction and Building Materials* 189: 1134–39. https://doi.org/10.1016/j.conbuildmat.2018.09.075.

LOIZEAU, J. -L, D. ARBOUILLE, S. SANTIAGO, and J. -P VERNET. 1994. “Evaluation of a Wide Range Laser Diffraction Grain Size Analyser for Use with Sediments.” *Sedimentology* 41 (2): 353–61. https://doi.org/10.1111/j.1365-3091.1994.tb01410.x.

Ma, Cong, Bing Chen, and Longzhu Chen. 2016. “Variables Controlling Strength Development of Self-Compacting Earth-Based Construction.” *Construction and Building Materials* 123: 336–45. https://doi.org/10.1016/j.conbuildmat.2016.07.017.

Mahvash, Siavash, Susana López-Querol, and Ali Bahadori-Jahromi. 2017. “Effect of Class F Fly Ash on Fine Sand Compaction through Soil Stabilization.” *Heliyon* 3 (3): e00274. https://doi.org/10.1016/j.heliyon.2017.e00274.

Majidi, Behzad. 2009. “Geopolymer Technology, from Fundamentals to Advanced Applications: A Review.” *Materials Technology* 24 (2): 79–87. https://doi.org/10.1179/175355509X449355.

Makusa, Gregory Paul. 2013. “State of the Art Review Soil Stabilization Methods and Materials in Engineering Practice.” *Luleå University of Technology, Luleå, Sweden*.

Mallikarjuna Rao G., Gunneswara Rao T.D., Siva Nagi Reddy M., and Rama Seshu D. 2019. “A

Study on the Strength and Performance of Geopolymer Concrete Subjected to Elevated Temperatures." In *Recent Advances in Structural Engineering, Volume 1*, 869–89. https://doi.org/https://doi.org/10.1007/978-981-13-0362-3_70.

Maniatidis, Vasilios, and Peter Walker. 2003. "A Review of Rammed Earth Construction." *Developing Rammed Earth for UK Housing*, no. May: 109. http://staff.bath.ac.uk/abspw/rammedearth/review.pdf.

———. 2008. "Structural Capacity of Rammed Earth in Compression." *Journal of Materials in Civil Engineering* 20 (3): 230–38. https://doi.org/10.1061/(asce)0899-1561(2008)20:3(230).

Marais, Paul, John Littlewood, and George Karani. 2015. "The Use of Polymer Stabilised Earth Foundations for Rammed Earth Construction." *Energy Procedia* 83: 464–73. https://doi.org/10.1016/j.egypro.2015.12.166.

Maskell, Daniel, Andrew Heath, and Peter Walker. 2014. "Geopolymer Stabilisation of Unfired Earth Masonry Units." *Key Engineering Materials* 600: 175–85. https://doi.org/10.4028/www.scientific.net/KEM.600.175.

Meek, A. H., and M. Elchalakani. 2019. "Life Cycle Assessment of Rammed Earth Made Using Alkaline Activated Industrial By-Products." *IOP Conference Series: Earth and Environmental Science* 323 (1). https://doi.org/10.1088/1755-1315/323/1/012143.

MFARD. 2016. "Programme Performance Report."

Morel, Jean Claude, Abalo Pkla, and Peter Walker. 2007. "Compressive Strength Testing of Compressed Earth Blocks." *Construction and Building Materials* 21 (2): 303–9. https://doi.org/10.1016/j.conbuildmat.2005.08.021.

Muhammad, Nurmunira, and Sumi Siddiqua. 2019. “Stabilization of Silty Sand Using Bentonite-magnesium-Alkalinization: Mechanical, Physicochemical and Microstructural Characterization.” *Applied Clay Science* 183 (October): 105325. https://doi.org/10.1016/j.clay.2019.105325.

Muhammad, Nurmunira, Sumi Siddiqua, M Asce, Nima Latifi, and M Asce. 2018. “Solidification of Subgrade Materials Using Magnesium Alkalinization : A Sustainable Additive for Construction” 30 (10): 1–13. https://doi.org/10.1061/(ASCE)MT.1943-5533.0002484.

Murmu, Anant Lal, Nupur Dhole, and Anjan Patel. 2020. “Stabilisation of Black Cotton Soil for Subgrade Application Using Fly Ash Geopolymer.” *Road Materials and Pavement Design* 21 (3): 867–85. https://doi.org/10.1080/14680629.2018.1530131.

Ochoa de Alda, Jesús A.G. 2008. “Feasibility of Recycling Pulp and Paper Mill Sludge in the Paper and Board Industries.” *Resources, Conservation and Recycling* 52 (7): 965–72. https://doi.org/10.1016/j.resconrec.2008.02.005.

Ogunye, F. O., and H. Boussabaine. 2002. “Development of a Rainfall Test Rig as an Aid in Soil Block Weathering Assessment.” *Construction and Building Materials* 16 (3): 173–80. https://doi.org/10.1016/S0950-0618(02)00010-7.

Omar Sore, Seick, Adamah Messan, Elodie Prud’homme, Gilles Escadeillas, and François Tsobnang. 2018. “Stabilization of Compressed Earth Blocks (CEBs) by Geopolymer Binder Based on Local Materials from Burkina Faso.” *Construction and Building Materials* 165: 333–45. https://doi.org/10.1016/j.conbuildmat.2018.01.051.

Palomo, A, P Krivenko, I Garcia-Lodeiro, E Kavalerova, O Maltseva, and A Fernández-Jiménez. 2014. “A Review on Alkaline Activation: New Analytical Perspectives ; Activación Alcalina:

Revisión y Nuevas Perspectivas de Análisis." *Materiales de Construcción* 64 (315): 22. https://doi.org/10.3989/mc.2014.00314.

Pitman, Rona M. 2006. "Wood Ash Use in Forestry - A Review of the Environmental Impacts." *Forestry* 79 (5): 563–88. https://doi.org/10.1093/forestry/cpl041.

Preethi, R. K., and B. V. Venkatarama Reddy. 2020. "Experimental Investigations on Geopolymer Stabilised Compressed Earth Products." *Construction and Building Materials* 257: 119563. https://doi.org/10.1016/j.conbuildmat.2020.119563.

Siddiqua, S., J Blatz, and G. Siemens. 2011. "Evaluation of the Impact of Pore Fluid Chemistry on the Hydromechanical Behaviour of Clay-Based Sealing Materials." *Canadian Geotechnical Journal.* 48(2): 199–213. https://doi.org/https://doi.org/10.1139/T10-064.

Siddiqua, Sumi, and Priscila N.M. Barreto. 2018. "Chemical Stabilization of Rammed Earth Using Calcium Carbide Residue and Fly Ash." *Construction and Building Materials* 169: 364–71. https://doi.org/10.1016/j.conbuildmat.2018.02.209.

Siddiqua, Sumi, Greg Siemens, James Blatz, Alex Man, and Bee Fong Lim. 2014. "Influence of Pore Fluid Chemistry on the Mechanical Properties of Clay-Based Materials." *Geotechnical and Geological Engineering* 32 (4): 1029–42. https://doi.org/10.1007/s10706-014-9778-z.

Siddique, Rafat. 2009. "Utilization of Waste Materials and By-Products in Producing Controlled Low-Strength Materials." *Resources, Conservation and Recycling* 54 (1): 1–8. https://doi.org/10.1016/j.resconrec.2009.06.001.

———. 2012. "Utilization of Wood Ash in Concrete Manufacturing." *Resources, Conservation and Recycling* 67: 27–33. https://doi.org/10.1016/j.resconrec.2012.07.004.

Silva, Rui A, Daniel V Oliveira, Tiago Miranda, Nuno Cristelo, Maria C Escobar, and Edgar Soares. 2013. “Rammed Earth Construction with Granitic Residual Soils : The Case Study of Northern Portugal.” *Construction and Building Materials* 47: 181–91. https://doi.org/10.1016/j.conbuildmat.2013.05.047.

Simão, L., D. Hotza, F. Raupp-Pereira, J. A. Labrincha, and O. R.K. Montedo. 2018. “Wastes from Pulp and Paper Mills - A Review of Generation and Recycling Alternatives.” *Ceramica* 64 (371): 443–53. https://doi.org/10.1590/0366-69132018643712414.

Singh, B., G. Ishwarya, M. Gupta, and S. K. Bhattacharyya. 2015. “Geopolymer Concrete: A Review of Some Recent Developments.” *Construction and Building Materials* 85: 78–90. https://doi.org/10.1016/j.conbuildmat.2015.03.036.

Šķēls, Pēteris, Kaspars Bondars, Raitis Plonis, Viktors Haritonovs, and Andris Paeglītis. 2016. “Usage of Wood Fly Ash in Stabilization of Unbound Pavement Layers and Soils,” no. September: 122–25. https://doi.org/10.3846/13bsgc.2016.017.

Soebarto, Veronica. 2009. “Analysis of Indoor Performance of Houses Using Rammed Earth Walls.” *IBPSA 2009 - International Building Performance Simulation Association 2009*, 1530–37. https://www.engineeringvillage.com/share/document.url?mid=cpx_17fa65e13b8c077a32M54af2061377553&database=cpx.

Sotelo-Piña, Carlos, Elsa Nadia Aguilera-González, and Antonia Martínez-Luévanos. 2019. “Geopolymers: Past, Present, and Future of Low Carbon Footprint Eco-Materials.” *Handbook of Ecomaterials* 4: 2765–85. https://doi.org/10.1007/978-3-319-68255-6_54.

Soudani, Lucile, Monika Woloszyn, Antonin Fabbri, Jean Claude Morel, and Anne Cécile Grillet.

2017. “Energy Evaluation of Rammed Earth Walls Using Long Term In-Situ Measurements.” *Solar Energy* 141: 70–80. https://doi.org/10.1016/j.solener.2016.11.002.

Sridharan, Asuri, and Puvvadi Venkata Sivapullaiah. 2005. “Mini Compaction Test Apparatus for Fine Grained Soils.” *Geotechnical Testing Journal* 28 (3): 240–46. https://doi.org/10.1520/gtj12542.

Stanjek, H; Hausler W. 2004. “3-Basics of X-Ray Diffraction,” 107–19.

Taallah, Bachir, Abdelhamid Guettala, Salim Guettala, and Abdelouahed Kriker. 2014. “Mechanical Properties and Hygroscopicity Behavior of Compressed Earth Block Filled by Date Palm Fibers.” *Construction and Building Materials* 59: 161–68. https://doi.org/10.1016/j.conbuildmat.2014.02.058.

Taylor, P., R. J. Fuller, and M. B. Luther. 2008. “Energy Use and Thermal Comfort in a Rammed Earth Office Building.” *Energy and Buildings* 40 (5): 793–800. https://doi.org/10.1016/j.enbuild.2007.05.013.

Taylor, P., and M. B. Luther. 2004. “Evaluating Rammed Earth Walls: A Case Study.” *Solar Energy* 76 (1–3): 79–84. https://doi.org/10.1016/j.solener.2003.08.026.

Teixeira, E. R., A. Camões, and F. G. Branco. 2019. “Valorisation of Wood Fly Ash on Concrete.” *Resources, Conservation and Recycling* 145 (February): 292–310. https://doi.org/10.1016/j.resconrec.2019.02.028.

Toller, S., E. Kärrman, J. P. Gustafsson, and Y. Magnusson. 2009. “Environmental Assessment of Incinerator Residue Utilisation.” *Waste Management* 29 (7): 2071–77. https://doi.org/10.1016/j.wasman.2009.03.006.

Toufigh, Vahab, and Ehsan Kianfar. 2019. “The Effects of Stabilizers on the Thermal and the Mechanical Properties of Rammed Earth at Various Humidities and Their Environmental Impacts.” *Construction and Building Materials* 200: 616–29. https://doi.org/10.1016/j.conbuildmat.2018.12.050.

Udoeyo, Felix F, Hilary Inyang, David T Young, and Edmund Oparadu. 2006. “Potential of Wood Waste Ash as an Additive in Concrete.” *Journal of Materials in Civil Engineering* 18 (July/August): 605–11. https://doi.org/10.1061/_ASCE_0899-1561_2006_18:4_605.

Upadhyaya, S .B. Tiwari2; and G. Olgun3. 2016. “Static and Dynamic Properties of Compacted Soil-Cement Mixtures.” *Geotechnical and Structural Engineering Congress 2016*, 483–89.

Wayal, A., D. Purohit, and N. Ameta. 2012. “Dune Sand Stabilization Using Bentonite and Lime.” *Journal of Engineering Research and Studies* III (I): 58–60.